JOURNAL OF VIROLOGY, Feb. 2004, p. 2088–2099 Vol. 78, No. 4
0022-538X/04/$08.00+0 DOI: 10.1128/JVI.78.4.2088–2099.2004

Mutant PrP^{Sc} Conformers Induced by a Synthetic Peptide and Several Prion Strains

Patrick Tremblay,[1,2]†‡ Haydn L. Ball,[1,2]†§ Kiyotoshi Kaneko,[1]‖ Darlene Groth,[1] Ramanujan S. Hegde,[3]# Fred E. Cohen,[1,4,5] Stephen J. DeArmond,[1,3] Stanley B. Prusiner,[1,2,5]* and Jiri G. Safar[1,2]

Institute for Neurodegenerative Diseases[1] and Departments of Neurology,[2] Biochemistry and Biophysics,[5] Cellular and Molecular Pharmacology,[4] and Pathology,[3] University of California, San Francisco, California 94143

Received 6 August 2003/Accepted 15 October 2003

Gerstmann-Sträussler-Scheinker (GSS) disease is a dominantly inherited, human prion disease caused by a mutation in the prion protein (PrP) gene. One mutation causing GSS is P102L, denoted P101L in mouse PrP (MoPrP). In a line of transgenic mice denoted Tg2866, the P101L mutation in MoPrP produced neurodegeneration when expressed at high levels. $MoPrP^{Sc}$(P101L) was detected both by the conformation-dependent immunoassay and after protease digestion at 4°C. Transmission of prions from the brains of Tg2866 mice to those of Tg196 mice expressing low levels of MoPrP(P101L) was accompanied by accumulation of protease-resistant $MoPrP^{Sc}$(P101L) that had previously escaped detection due to its low concentration. This conformer exhibited characteristics similar to those found in brain tissue from GSS patients. Earlier, we demonstrated that a synthetic peptide harboring the P101L mutation and folded into a β-rich conformation initiates GSS in Tg196 mice (29). Here we report that this peptide-induced disease can be serially passaged in Tg196 mice and that the PrP conformers accompanying disease progression are conformationally indistinguishable from $MoPrP^{Sc}$(P101L) found in Tg2866 mice developing spontaneous prion disease. In contrast to GSS prions, the 301V, RML, and 139A prion strains produced large amounts of protease-resistant PrP^{Sc} in the brains of Tg196 mice. Our results argue that $MoPrP^{Sc}$(P101L) may exist in at least several different conformations, each of which is biologically active. Such conformations occurred spontaneously in Tg2866 mice expressing high levels of $MoPrP^{C}$(P101L) as well as in Tg196 mice expressing low levels of $MoPrP^{C}$(P101L) that were inoculated with brain extracts from ill Tg2866 mice, with a synthetic peptide with the P101L mutation and folded into a β-rich structure, or with prions recovered from sheep with scrapie or cattle with bovine spongiform encephalopathy.

The discovery that brain fractions enriched for prion infectivity contain a protein ($rPrP^{Sc}$) that is resistant to limited proteolytic digestion advanced prion research (8, 37). N-terminal truncation of $rPrP^{Sc}$ produced a protease-resistant fragment, denoted PrP 27-30, that is readily measured by Western blotting, enzyme-linked immunosorbent assay, or immunohistochemistry. The measurement of PrP^{Sc} was dramatically changed with the development of the conformation-dependent immunoassay (CDI), which permitted detection of full-length $rPrP^{Sc}$ as well as previously unrecognized protease-sensitive forms of PrP^{Sc} (39).

The CDI depends on using anti-PrP antibodies that react with an epitope exposed in native PrP^{C} but that do not bind to native PrP^{Sc}. Upon denaturation, the buried epitope in PrP^{Sc} becomes exposed and readily reacts with anti-PrP antibodies. Using the CDI, we discovered that most PrP^{Sc} is protease sensitive, which we designate $sPrP^{Sc}$. Whether $sPrP^{Sc}$ is an intermediate in the formation of $rPrP^{Sc}$ remains to be determined. In Syrian hamsters inoculated with eight different strains of prions, the ratio of $rPrP^{Sc}$ to $sPrP^{Sc}$ was different for each strain and the concentration of $sPrP^{Sc}$ was proportional to the length of the incubation time (39).

In earlier studies, transgenic (Tg) mice, denoted Tg2866, expressing high levels of PrP(P101L) were used to model Gerstmann-Sträussler-Scheinker (GSS) disease caused by the P102L point mutation. In the brains of several lines of mice expressing high levels of PrP(P101L), no $rPrP^{Sc}$(P101L) was detectable (26, 27, 47). This was particularly perplexing since these Tg mice expressing high levels of PrP(P101L) developed all facets of prion-induced neurodegeneration, including multicentric PrP amyloid plaques. Moreover, brain extracts from ill Tg2866 mice transmitted disease to Tg196 mice expressing low levels of PrP(P101L) that infrequently developed spontaneous neurodegeneration (29).

In humans with GSS, several different mutations of the PrP gene (*PRNP*) resulting in nonconservative amino acid substitutions have been identified (23). In these patients, the clinical presentation, disease course, and amounts of $rPrP^{Sc}$ in the brain are variable. Brain extracts from humans who died of GSS were inoculated into apes and monkeys, but the transmission rates were not correlated with the levels of PrP^{Sc} in the inoculum (1, 2, 9, 32). In a limited study, GSS(P102L) was transmitted to Tg mice expressing a chimeric mouse-human (MHu2 M) PrP transgene carrying the P102L mutation but not

* Corresponding author. Mailing address: Institute for Neurodegenerative Diseases, University of California, Box 0518, San Francisco, CA 94143-0518. Phone: (415) 476-4482. Fax: (415) 476-8386. E-mail: stanley@itsa.ucsf.edu.

† These authors contributed equally to this work.

‡ Present address: Neurochem Inc., St. Laurent, QC H4S 2A1, Canada.

§ Present address: University of Texas Southwestern Medical Center, Dallas, TX 75390.

‖ Present address: National Center of Neurology and Psychiatry and Core Research for Evolutional Science and Technology, Kodaira, Tokyo 187-8502, Japan.

Present address: National Cancer Institute, Bethesda, MD 20892.

TABLE 1. Characteristics of PrP(P101L) isoforms

Characteristic	Isoform[a]		
	PrP^{c}(P101L)	$sPrP^{Sc}$(P101L)	$rPrP^{Sc}$(P101L)
PrP epitopes (residues 90–125) in native state	Exposed	Buried	Buried
Precipitatable by PTA	−	+	+
Digestion with PK at 37°C ("PK")	Dipeptides, tripeptides	Dipeptides, tripeptides	PrP 27–30
Digestion with PK at 4°C ("cold PK")	Dipeptides, tripeptides	PrP 22–24	PrP 27–30
Infectious	−	?	+

[a] ?, unknown; +, positive; −, negative.

to Tg mice expressing MHu2M PrP without the mutation (47). In another study, GSS(P102L) human prions were transmitted to Tg mice expressing MoPrP(P101L) in which the transgene was incorporated through gene replacement (31). The use of gene replacement permits all of the regulatory elements that control the wild-type (wt) MoPrP gene to modulate the expression of MoPrP(P101L). In these mice, the expression level of MoPrP(P101L) in brain is likely to be similar to that in Tg196 mice.

When we synthesized a 55-mer MoPrP peptide composed of residues 89 to 143 containing the P101L mutation and folded it under conditions favoring a β-structure, it induced neurodegeneration in Tg196 mice (29). When the peptide was not folded into a β-structure, it did not produce disease in Tg196 mice. We report here that the peptide-initiated disease in Tg196 mice could be serially transmitted to other Tg196 mice using brain extracts from the peptide-inoculated Tg196 mice. Using procedures derived from the CDI, brain extracts from inoculated Tg196 mice were found to contain $sPrP^{Sc}$(P101L), from which a 22- to 24-kDa PrP fragment was generated by limited digestion with proteinase K (PK) at 4°C and selective precipitation with phosphotungstate (PTA) (25, 39). In the interest of clarity, we have designated digestion at 4°C as "cold PK" and simply refer to standard digestion at 37°C as "PK." To aid in distinguishing $rPrP^{Sc}$(P101L) from $sPrP^{Sc}$(P101L), their properties based on the work reported here and in other previously published papers are listed in Table 1 (39, 40).

In addition to inoculating Tg196 mice with brain extracts containing $sPrP^{Sc}$(P101L) or with the MoPrP(89-143,P101L) peptide, we inoculated Tg196 with several strains of prions carrying wt $MoPrP^{Sc}$-A or $MoPrP^{Sc}$-B. The 301V strain carrying wt $MoPrP^{Sc}$-B (22) exhibited similar abbreviated incubation times in both Tg196 mice and $Prnp^{b/b}$ mice. In contrast, the RML and 139A strains carrying wt $MoPrP^{Sc}$-A showed prolonged incubation times in both Tg196 and $Prnp^{b/b}$ mice (12, 33). Regardless of the host mouse strain, the 301V, RML, and 139A prion strains produced large amounts of $rPrP^{Sc}$ in the brains of inoculated mice. Thus, the discovery of $sPrP^{Sc}$ has for the first time provided a molecular signature for GSS prions that either arise spontaneously in mice or are induced by a synthetic peptide carrying the GSS mutation.

MATERIALS AND METHODS

Source of laboratory animals. The results reported here were derived from studies using Tg(MoPrP,P101L)196/$Prnp^{0/0}$, Tg(MoPrP,P101L)2866/$Prnp^{0/0}$, Tg(MoPrP,P101L)2247/$Prnp^{0/0}$, Tg(MoPrP)4053/$Prnp^{+/+}$, Tg(MHu2M)5378/$Prnp^{0/0}$, and Tg(MHu2MPrP,P102L)69/$Prnp^{0/0}$ mice; these Tg lines are described in detail elsewhere (27, 47, 48). All PrP-deficient animals originated from Zrch $Prnp^{0/0}$ mice (11). Transgenic lines were maintained by breeding with FVB $Prnp^{0/0}$, except for Tg(MoPrP)4053/$Prnp^{+/+}$, in which the endogenous *Prnp* gene was maintained by breeding with FVB mice (Charles River Laboratories, Hollister, Calif.). Swiss CD-1 mice, which express $Prnp^{a}$, were obtained from Charles River Laboratories, and B6.I mice, which express $Prnp^{b}$, were a generous gift from G. Carlson (12). Rabbits were obtained from Western Oregon Rabbit Company (Philomath, Ore.).

Transmission studies. The RML prion strain was derived from the Chandler isolate (14) passaged in CD-1 mice. The mouse 139A prion strain, originally isolated after more than 20 passages in mice, was obtained from R. Carp (21) and serially propagated in C57BL ($Prnp^{a/a}$) mice obtained from Charles River Laboratories. The 301V prion strain, originally isolated from a cow infected with bovine spongiform encephalopathy (BSE), was obtained from H. Fraser (10) and maintained by serial passaging in B6.I mice. Brains from ill, MoPrP(89-143, P101L) peptide-inoculated Tg196 mice were obtained from previously reported experiments (29). Ten-percent (wt/vol) brain homogenates (BH) were obtained by 10 serial extrusions through 18-, 20-, and 22-gauge needles in phosphate-buffered saline (PBS) (pH 7.4). Mice were inoculated intracerebrally (i.c.) with 30 μl of 1% BH (Table 2) or with a clarified 0.5% BH (Table 3) using a 27-gauge, disposable hypodermic syringe. Alternatively, following PTA precipitation of 1 ml of BH, pellets were resuspended in 500 μl of diluent (PBS) before i.c. inoculation (Table 3). Disease diagnosis was carried out biweekly, and animals were sacrificed following evidence of progressive neurologic dysfunction (13, 41).

Treatment of brain homogenates. For biochemical analysis only, 10% BH samples were prepared in Ca^{++}- and Mg^{++}-free PBS by homogenization (three strokes of 15 s each) with a PowerGen 125 homogenizer (Fisher Scientific). Homogenates were clarified by centrifugation at 500 × *g* for 5 min on a tabletop centrifuge. Supernatants were subjected to cold PK or PK digestion alone or in conjunction with PTA precipitation. For PK digestion, 5% BH samples were incubated with 25 μg of PK (Gibco BRL no. 25530-015; Invitrogen, Carlsbad, Calif.)/ml for 1 h at 37°C. PK activity was blocked using a protease inhibitor (PI) cocktail composed of 2 μg of aprotinin and leupeptin/ml and 0.2 mM phenylmethylsulfonyl fluoride. For cold PK digestion, clarified 10% BH containing 1% NP-40 was incubated with 250 μg of PK/ml for 1 h on ice. Samples were treated with PI (200 μg of aprotinin and leupeptin/ml and 5 mM phenylmethylsulfonyl fluoride), transferred to five volumes of preheated PK inactivation buffer (1% sodium dodecyl sulfate [SDS], 0.1 M Tris-HCl [pH 8.9]), and incubated at 100°C for 2 min. For cold PK followed by PTA precipitation, 10% BH were treated with cold PK, and the reaction was blocked using PI. Samples were diluted with one volume of PBS–4% Sarkosyl and PTA precipitated. For ultracentrifugation, 1 ml of these samples was centrifuged at 100,000 × *g* for 1 h at 4°C. Alternatively, 1 ml was precipitated with PTA by adjusting samples to 0.3% PTA–2.5 mM $MgCl_2$, incubated at 37°C for 1 h, and centrifuged at 16,000 × *g* for 30 min. Pellets were resuspended in PBS with PI and 0.2% Sarkosyl.

For Western blot analysis, samples were diluted with one volume of 0.1 M Tris (pH 6.8)–2% mercaptoethanol–2% NP-40 and subjected to 7.2 U of PNGase F1 per 100 μg of total protein at 37°C overnight, according to the manufacturer's recommendations (Boehringer-Mannheim, Mannheim, Germany). Proteins were precipitated with 25% trichloroacetic acid and washed with acetone. Pellets were resuspended in 1% SDS–0.1 M Tris-HCl (pH 8.9) buffer for loading on an SDS polyacrylamide gel.

Immunological reagents. To take advantage of the CDI and characterize the conformational transitions associated with PrP(P101L), we sought to identify antibodies that recognize epitopes in the region of MoPrP(P101L) located between residues 89 and 143. Surprisingly, all previously described candidate antibodies for this assay (including recombinant fragment antibody D13 [35] and polyclonal antiserum 9095 [42]), which recognize wt MoPrP within these boundaries, poorly recognized MoPrP(P101L) by Western blotting (data not shown). Therefore, a polyclonal antiserum was raised in rabbits using a random-coil

TABLE 2. Effect of the P101L mutation on the generation and transmission of infectious prions

Inoculum[a,b]	Recipients[b]	PrP^C expression level[c]	Time to disease (days ± SEM)	n/n_0[d]
None	Tg(MoPrP,P101L)196	1	552 ± 34	9/32
None	Tg(MoPrP,P101L)2866	8	132 ± 2	19/19
Tg(MoPrP,P101L)2866	CD-1	1	>700	0/8
Tg(MoPrP,P101L)2866	Tg(MoPrP-A)4053	8	>700	0/7
Tg(MoPrP,P101L)2866	Tg(MoPrP,P101L)196	1	305 ± 17	10/10
Tg(MoPrP,P101L)2866	Tg(MoPrP,P101L)196	1	263 ± 12	8/8
Tg196(2866)	Tg(MoPrP,P101L)196	1	351 ± 13	8/8
Non-β-MoPrP(89-143,P101L)[e]	Tg(MoPrP,P101L)196	1	632	1/8
β-MoPrP(89-143,P101L)[e,f]	Tg(MoPrP,P101L)196	1	360 ± 30	20/20
Tg196(β-MoPrP(89-143,P101L))[g]	Tg(MoPrP,P101L)196	1	349 ± 8	8/8
Tg196(β-MoPrP(89-143,P101L))[g]	Tg(MoPrP,P101L)196	1	351 ± 9	9/9
Tg196(β-MoPrP(89-143,P101L))[g]	Tg(MoPrP,P101L)196	1	327 ± 9	8/8
CD-1(RML)	CD-1	1	131 ± 0	29/29
CD-1(RML)[f]	Tg(MoPrP,P101L)196	1	229 ± 6	6/6
Tg196(RML)[g]	Tg(MoPrP,P101L)196	1	175 ± 1	7/7
Tg196(RML)[g]	Tg(MoPrP,P101L)196	1	186 ± 3	9/9
C57(139A)	CD-1	1	144 ± 2	14/14
C57(139A)[f]	Tg(MoPrP,P101L)196	1	425 ± 4	9/9
Tg196(139A)[g]	Tg(MoPrP,P101L)196	1	179 ± 8	9/9
Tg196(139A)[g]	Tg(MoPrP,P101L)196	1	198 ± 6	9/9
CD-1(301V)	CD-1	1	230 ± 3	10/10
CD-1(301V)	B6.I	1	132 ± 1	10/10
B6.I(301V)	B6.I	1	116 ± 1	17/17
B6.I(301V)	CD-1	1	224 ± 5	8/8
B6.I(301V)[f]	Tg(MoPrP,P101L)196	1	113 ± 4	9/9
B6.I(301V)[f]	Tg(MoPrP,P101L)196	1	127 ± 2	3/3
Tg196(301V)[g]	Tg(MoPrP,P101L)196	1	130 ± 3	5/5
Tg196(301V)[g]	Tg(MoPrP,P101L)196	1	129 ± 1	4/4

[a] Original prion inocula (RML, 139A, 301V) were obtained from *Prnp*^{a} (C57, CD-1) and/or *Prnp*^{b} mice (B6.I) or from spontaneously ill Tg(MoPrP,P101L)2866 mice. Homogenates used for transmissions originated from spontaneously ill or prion-inoculated mice at time of disease onset. The prion strain is shown in parentheses and the text preceding the parenthesis indicate the host in which it was last propagated.

[b] All Tg(MoPrP,P101L) mice were *Prnp*$^{0/0}$.

[c] Levels of PrP^C expression are compared with that of adult, wt FVB mice.

[d] Number of ill mice (n) over the total number of mice under observation (n_0).

[e] Data from reference 29.

[f] These inoculations correspond to the primary transmissions.

[g] Inocula used for these secondary transmissions were prepared from brains obtained in the primary transmissions from spontaneously ill or prion-inoculated mice at time of disease onset.

MoPrP(89-143,P101L) peptide. Four rabbits preselected for the low reactivity of their sera against homogenates from wt mouse brains were immunized subcutaneously with 1 ml of the MoPrP(89-143,P101L) peptide (250 μg/ml in PBS-RIBI adjuvant). This procedure was performed three times at 3-week intervals. Rabbits were bled 14 days after the final immunization procedure, and their sera were tested by Western blotting for reactivity against MoPrP(P101L). The serum from rabbit 5449 displayed strong reactivity against MoPrP(P101L), MHu2M(P102L), and HuPrP(P102L) but not against wt controls (Fig. 1). The epitope mapping with overlapping synthetic peptides demonstrated two dominant epitopes: one between residues 94 and 108 and a second between residues 129 and 143 (data not shown). Western blot analyses were performed as previously described (4), using anti-PrP 3F4 monoclonal antibody at a 1:2,500 dilution (30), RO73 polyclonal antiserum at a 1:5,000 dilution (43), or 5449 polyclonal antiserum at a 1:1,000 dilution. Blots were developed using the enhanced chemiluminescence system (Amersham Life Science, Arlington Heights, Ill.).

Detection of PrP^{Sc} by the CDI. Samples were processed for the CDI using time-resolved fluorescence spectroscopy, as previously described (39). Samples were split into two aliquots, one of which was kept untreated (native) while the second (denatured) was treated with one volume of 8 M guanidinium hydrochloride and heated at 80°C for 5 min. Both aliquots were further diluted 20-fold with a water-PI mixture. Samples were loaded in triplicates on 96-well polystyrene microplates (OptiPlate HTRF-96; Perkin-Elmer, Boston, Mass.) that were either precoated with the R1 recombinant fragment antibody (35) or preactivated with gluteraldehyde (0.2% in PBS [pH 7.4]; 2 h). The plates were incubated for 2 h at room temperature and blocked overnight with Tris-buffered saline (20 mM Tris-HCl [pH 7.5], 1% bovine serum albumen, 6% sorbitol) at 4°C. Primary antibodies were then added to the plates. The anti-PrP RO73 polyclonal antiserum was used at a 1:1,000 dilution with R1-coated plates, and the 5449 polyclonal antiserum was used at a 1:1,000 dilution on gluteraldehyde-activated plates, for 2 h at 37°C. Plates were washed three times with TBS–0.05% Tween 20 and incubated for 1 h with a Europium (Eu)-labeled, anti-rabbit antibody (Delfia, no. AD0105; 1:5,000). Plates were washed seven times with a Eu enhancement solution (Wallac, Turku, Finland) and read using a Discovery fluorescence detector (Perkin-Elmer). The difference in binding between the native (N) and denatured (D) states is expressed as the D:N ratio. A mathematical model was developed to calculate the β-sheet content in PrP using these values (39). The concentration of PrP in the samples was calculated from calibration curves generated with the β-rich recombinant MoPrP(89-231) for RO73 or with synthetic MoPrP(89-143,P101L) for 5449. The signal obtained from normal Tg(MoPrP,P101L)196/*Prnp*$^{0/0}$ was used as an internal reference between plates.

Histopathological procedures. Brains were removed from euthanatized animals shortly after death and were frozen on dry ice or immersion fixed in 10% buffered formalin for inclusion in paraffin. Histoblots were performed on 10-μm, frozen coronal sections, transferred to a nitrocellulose membrane, and processed for immunohistochemistry using anti-PrP RO73 polyclonal antiserum, as previously described (45). Eight-micrometer paraffin sections were stained with hematoxylin and eosin for evaluation of neurodegenerative changes. Evaluation of reactive astrocytic gliosis was performed by immunostaining of glial fibrillary

TABLE 3. Propagation of GSS(P101L) prions in transgenic mice

Inoculum[a]	Treatment	Time to disease (days ± SEM)	n/n_0[b]	Time elapsed (days)
Tg196[c]	None	478 ± 37	6/7	>500
	PTA	432	1/8	>550
	PK/PTA	468 ± 22	2/9	>500
	PTA/PK	483	1/9	>500
Tg2866[d]	None	305 ± 17	10/10	
	PTA	278 ± 16	10/10	
	PK/PTA	262 ± 12	8/8	
	PTA/PK	226 ± 8	10/10	
Tg196(2866)[e]	None	351 ± 13	8/8	
	PTA	294 ± 4	9/9	
	PK/PTA	286 ± 3	10/10	
	PTA/PK	279 ± 7	9/9	
Tg196(196(301V))[f]	None	144 ± 4	6/7	>550
	PTA	148 ± 6	7/7	
	PK/PTA	126 ± 3	5/5	
	PTA/PK	131 ± 3	8/8	

[a] All transmissions were carried out using Tg(MoPrP,P101L)196/$Prnp^{0/0}$ mice as recipients. For each inoculum series, a pool of at least three brain homogenates was split among the following treatments: none, untreated; PTA, sodium phosphotungstate precipitation; PK/PTA, PK digestion followed by PTA precipitation; PTA/PK, PTA precipitation followed by PK digestion.

[b] Number of ill animals (n) over number of animals under observation (n_0).

[c] Samples from clinically normal Tg(MoPrP,P101L)196/$Prnp^{0/0}$ mice age-matched with ill Tg196(2866) mice at ~300 days of age.

[d] Tg2866 corresponds to spontaneously ill Tg(MoPrP,P101L)2866/$Prnp^{0/0}$ mice at ~130 days of age.

[e] Tg196(2866) corresponds to ill Tg(MoPrP,P101L)196/$Prnp^{0/0}$ mice (~300 days of age) following inoculation with brain homogenates from spontaneously ill Tg2866 mice.

[f] Tg196(196(301V)) inoculum was obtained from the secondary transmission of 301V prions into Tg(MoPrP,P101L)196/$Prnp^{0/0}$ mice (see Table 1).

acidic protein using a rabbit antiserum (Dako, Carpinteria, Calif.), as previously described (34). Hydrolytic autoclaving immunodetections were carried out on paraffin-embedded sections (34).

RESULTS

Serial passage of peptide-induced GSS in Tg196 mice. In earlier studies, we reported that the i.c. inoculation of a 55-mer peptide, designated MoPrP(89-143,P101L), carrying the P101L mutation and folded into β-rich conformation, induces central nervous system (CNS) degeneration in Tg196 mice (Table 2) (29). All of the Tg196 mice succumbed to disease at ~360 days after inoculation with this peptide. Approximately 30% of uninoculated Tg196 mice developed disease at ~550 days of age.

Brain homogenates from three Tg196 mice that developed disease after peptide inoculation were inoculated into three separate groups of Tg196 mice. All of the mice developed disease, with similar mean incubation periods of 327 days, 349 days, and 351 days (Table 2). These results argue convincingly that the β-rich MoPrP(89-143,P101L) peptide induces the accumulation of infectious prions that can be serially propagated in Tg196 mice. We conclude from these findings that the β-rich 55-mer peptide either initiated the formation of de novo GSS prions in the host or is itself a synthetic prion.

Overexpression of MoPrP(P101L) induces spontaneous neurodegeneration. When high levels of MoPrP(P101L) were expressed in the brains of Tg2866 mice, mice developed spontaneous neurodegeneration at ~130 days of age. Extracts prepared from the brains of two ill Tg2866 mice inoculated into two groups of Tg196 mice caused disease in 263 days and 305 days.

Neuropathology of Tg196 mice. Often, prion strains can be distinguished by the histopathological distribution of lesions, the pattern of PrP^{Sc} accumulation, and the presence and type of amyloid plaques produced in infected brains (20) (Fig. 2). Tg196 mice inoculated with brain extracts prepared from spontaneously ill Tg2866 mice showed neuropathologic changes similar to those of Tg196 mice inoculated with the MoPrP (89-143,P101L) peptide (Fig. 2B and C). Tg196 mice that developed disease after inoculation with the MoPrP(89-143,

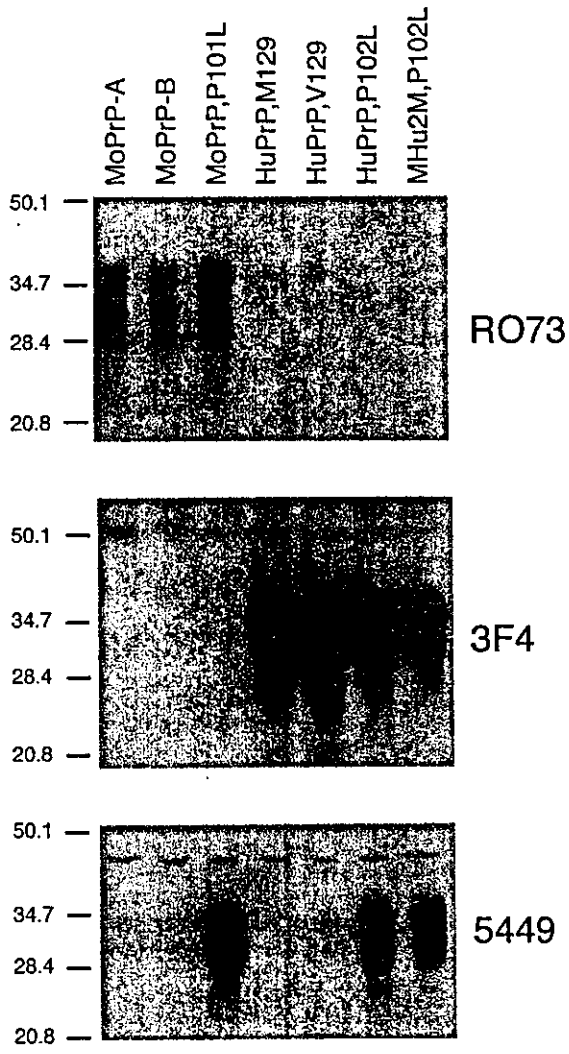

FIG. 1. Selective immunoreactivity of rabbit polyclonal antiserum 5449 raised against the MoPrP(89-143,P101L) peptide with PrPs carrying the P101L mutation. Brain homogenates (20 μg of total protein per lane) from mice expressing wt MoPrP-A (FVB), wt MoPrP-B (ILn/J), MoPrP(P101L) [Tg(MoPrP,P101L)196/$Prnp^{0/0}$], HuPrP(M129) [Tg(HuPrP,M129)440/$Prnp^{0/0}$], HuPrP(V129) [Tg(HuPrP,V129)152/$Prnp^{0/0}$], HuPrP(P102L) [Tg(HuPrP,P102L)7/$Prnp^{0/0}$], and MHu2M(P102L) [Tg(MHu2M,P102L)69/$Prnp^{0/0}$] were processed. Western blots were developed using the anti-PrP(P101L) 5449 polyclonal antiserum, and for comparison, with the anti-PrP RO73 polyclonal antiserum and the 3F4 monoclonal antibody. The apparent molecular weights of the migrated fragments are shown in thousands.

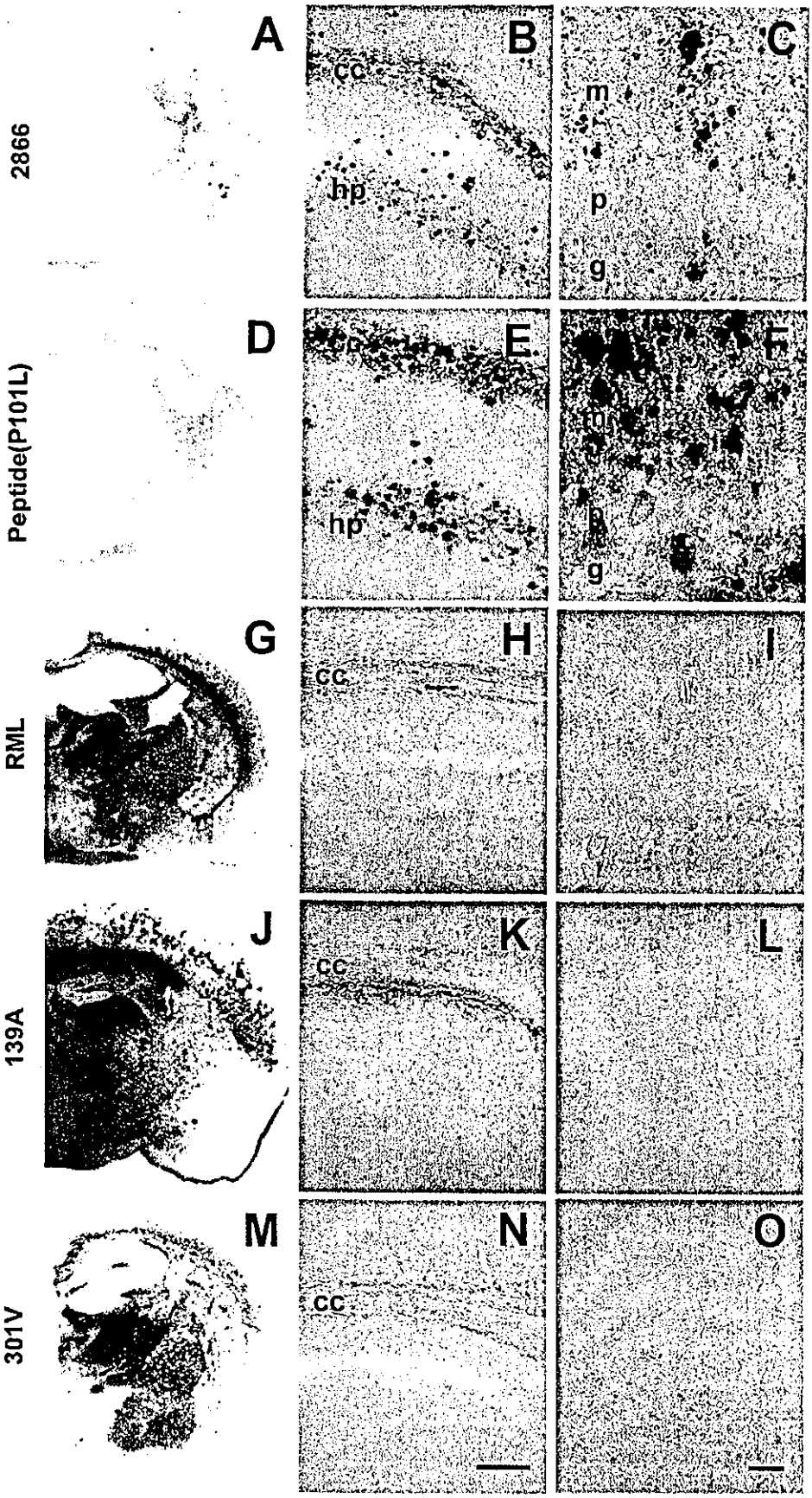
A
B
C
2866
cc
hp
m
p
g
D
E
F
Peptide(P101L)
cc
hp
m
p
g
G
H
I
RML
cc
J
K
L
139A
cc
M
N
O
301V
cc

P101L) peptide showed numerous large (70 μm), multicentric, GSS-like plaques in the neocortex, hippocampus, corpus callosum, caudate nucleus, globus pallidus, and cerebellar cortex (Fig. 2E and F). All of these plaques stained with anti-PrP antibodies. Severe spongiform changes and astrocytic gliosis associated with the loss of granule cells and numerous immature, GSS-like amyloid plaques were found in the cerebellum.

Prion strains from wt mice. Tg196 mice were susceptible to prion strains isolated in wt mice. RML and 139A strains were isolated from sheep with naturally occurring scrapie and passaged in $Prnp^{a/a}$ mice. In CD-1 ($Prnp^{a/a}$) mice, the incubation periods for RML and 139A prions were ~130 and ~145 days, respectively. When RML and 139A prions were inoculated into Tg196 mice, prolonged incubation periods of ~230 and ~425 days, respectively, were observed (Table 2); on second passage, the incubation times shortened to ~180 days and ~190 days, respectively. 301V prions were isolated from cattle with BSE by passage in $Prnp^{b/b}$ mice. When 301V prions were transmitted from $Prnp^{b/b}$ mice to Tg196 mice, incubation periods of ~120 days and ~115 days were observed on first and second passage, respectively. 301V prions have similar incubation periods in $Prnp^{b/b}$ and Tg196 mice but produce incubation periods of ~230 days in CD-1 mice.

These findings suggest that the P101L mutation creates a transmission barrier for propagation of the RML and 139A prion strains previously passaged in $Prnp^{a/a}$ mice. In contrast, the mutation poses no transmission barrier for 301V prions previously passaged in $Prnp^{b/b}$ mice. Taken together, our findings argue that the P101L mutation has an effect on incubation times similar to that of the L108F and T189V substitutions encoded in mouse $Prnp^{b}$ (49).

Intracerebral inoculation of Tg196 mice with the RML, 139A, and 301V prions resulted in neuropathological changes typical of experimental scrapie. The accumulation of $rPrP^{Sc}$ was evident using the histoblot method (Fig. 2G, J, and M) and vacuolation of the gray matter localized with sites of PrP^{Sc} accumulation (data not shown). Small (25 μm), subcallosal PrP plaques were also present in the brains of RML- and 139A-inoculated animals (Fig. 2H to I, K to L, and N to O). No plaques were found in the cerebella of mice inoculated with any of these three prion strains (Figs. 2I, L, and O).

Histoblotting revealed that each of the three prion strains produced a unique distribution of $rPrP^{Sc}$ in the gray and/or white matter (Fig. 2G, J, and M). For example, 139A prions produced intense PrP^{Sc} immunostaining in the hippocampus, but inoculation with RML and 301V prions did not produce PrP^{Sc} deposits in this region. Inoculation with RML prions resulted in a mild degree of vacuolation in layers IV through VI of the neocortex (data not shown) that correlated well with the medium-intensity immunostaining for PrP^{Sc} confined to the inner half of the neocortex (Fig. 2G). In animals inoculated with the 301V strain, immunostaining was not observed in the neocortex (Fig. 2M) and vacuolation was not detected (data not shown).

Biochemical detection of MoPrP(P101L) conformers. Earlier attempts using PK digestion for prolonged durations failed to identify altered forms of MoPrP(P101L) that feature in neurodegeneration. Therefore, we employed two new approaches. First, we took advantage of the ability of PTA to differentially precipitate PrP^{Sc} while leaving PrP^{C} in the supernatant fraction. Second, we employed alternative conditions for PK digestions by lowering the temperature to 4°C, a condition employed previously to demonstrate alterative forms that mutant PrPs can adopt (25). The protease resistance of MoPrP(P101L) conformers was probed using two different protocols: (i) digestion with 25 μg of PK/ml for 1 h at 37°C and (ii) digestion with 250 μg of PK/ml for 1 h at 4°C. In previous studies, we designated the latter protocol using digestion at 4°C as "mild PK" to distinguish it from the "harsh PK" protocol with digestion at 37°C (25). In the interest of clarity, here we designate digestion at 4°C as "cold PK" and simply refer to digestion at 37°C as "PK" (Table 1).

As previously described, $rPrP^{Sc}$(P101L) was undetectable in the brains of spontaneously ill Tg2886 or ill Tg196 mice after inoculation with mouse GSS(P101L) prions (27, 28, 47). Similar results were obtained with Tg196 mice inoculated with the β-rich MoPrP(89-143,P101L) peptide and in subsequent passages (Fig. 3F) (29). Low levels of $rPrP^{Sc}$(P101L) were detected in spontaneously ill Tg2866 mice only when samples were concentrated by ultracentrifugation (Fig. 3C). These low levels of $rPrP^{Sc}$(P101L) in brain homogenates from Tg mice infected with GSS(P101L) prions or the β-rich MoPrP(89-143,P101L) peptide contrast with the high levels of $rPrP^{Sc}$(P101L) in Tg196 mice inoculated with RML, 139A, or 301V prions (Fig. 3C and data not shown).

Traces of PTA-precipitable PrP were found in uninoculated, age-matched, control Tg196 and Tg(MoPrP-A)4053/$Prnp^{0/0}$ mice (Fig. 3B). In contrast, the PTA-precipitable PrP fraction was severalfold greater in the brains of spontaneously ill Tg2866 mice and in Tg196 mice inoculated with brain homogenates from spontaneously ill Tg2866 mice.

In the brains of spontaneously ill Tg2866 mice, high levels of a PrP^{Sc} fragment migrating to 22 to 24 kDa on Western blots was detected by cold PK digestion; PrP 22-24 is the cold PK-resistant fragment of $sPrP^{Sc}$(P101L) (Table 1). PrP 22-24 was also found in Tg196 mice following inoculation with mouse GSS(P101L) prions or with the β-rich MoPrP(89-143,P101L) peptide after first and second passages (Fig. 3D to F). The cold PK-resistant signal was stronger after PTA precipitation. Normal, age-matched Tg196 mice (~350 days of age) and Tg4053

FIG. 2. GSS-like neuropathological features in the absence of PK-resistant PrP^{Sc} in spontaneous and synthetic peptide-induced prion disease in Tg mice expressing the MoPrP(P101L) allele. The analyzed brains are from Tg(MoPrP,P101L)196/$Prnp^{0/0}$ mice inoculated with prions from spontaneously ill Tg(MoPrP,P101L)2866/$Prnp^{0/0}$ mice (A, B, and C), β-rich MoPrP(89–143,P101L) peptide (D, E, and F), or for comparison, with RML (G, H, and I), 139A (J, K, and L), or 301V (M, N, and O) prions. Distribution of $rPrP^{Sc}$ was determined by histoblotting (A, D, G, J, and M), and PrP-immunoreactive plaques were detected by hydrolytic autoclaving in the hippocampus (B, E, H, K, and N) and cerebellum (C, F, I, L, and O). Abbreviations: cc, corpus callosum; g, granule cell layer; hp, stratum radiatum of the CA1 region of the hippocampus; m, molecular layer; p, Purkinje cell layer. The bar in panel N represents 100 μm and applies to panels B, E, H, and K; The bar in panel O represents 30 μm and applies to panels C, F, I, and L.

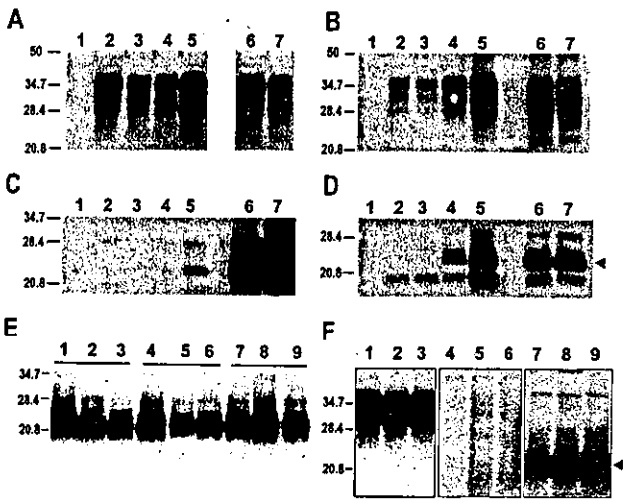

FIG. 3. Serial passage of aberrant PrP conformers in Tg(MoPrP, P101L) mice, detected by selective PTA precipitation and cold PK treatment. The 22- to 24-kDa PrP fragment (arrowheads) was found exclusively in Tg196 mice following inoculation with mouse GSS(P101L) prions or the β-rich MoPrP(89-143,P101L) peptide after both first and second passages. (A to D) Brain homogenates from uninoculated $Prnp^{0/0}$ mice (lane 1), Tg(MoPrP-A)4053/$Prnp^{0/0}$ mice (lane 2), uninoculated Tg(MoPrP,P101L)196/$Prnp^{0/0}$ mice (lane 3), Tg196 mice inoculated with brain homogenates from ill Tg2866 mice (lane 4), spontaneously ill Tg2866 mice (lane 5), Tg196 mice inoculated with RML prions (lane 6), or Tg196 mice inoculated with 301V prions (lane 7) are shown. Brain homogenates were untreated (A), precipitated with PTA (B), PK digested and subjected to ultracentrifugation (C), or subjected to cold PK digestion and precipitated with PTA (D). (E) Brain homogenates subjected to cold PK digestion and PTA precipitation from spontaneously ill Tg2866 mice (lanes 1 to 3), Tg196 mice inoculated with brain homogenates of diseased Tg2866 mice (lanes 4 to 6), or second passage of Tg2866 brain homogenates in Tg196 mice (lanes 7 to 9). (F) Brain homogenates from Tg196 mice inoculated with brain homogenates from ill Tg2866 mice (lanes 1, 4, and 7), β-rich MoPrP(89-134,P101L) peptide (lanes 2, 5, and 8), or second passage of MoPrP(89-134,P101L) peptide into Tg196 mice (lanes 3, 6, and 9). Samples were untreated (lanes 1 to 3), PK digested and ultracentrifuged (lanes 4 to 6), or subjected to cold PK digestion and PTA precipitation (lanes 7 to 9). Blots were developed using anti-PrP RO73 (A to D) or anti-PrP(P101L) 5449 polyclonal antisera raised against a random-coil MoPrP(89–143,P101L) peptide (E and F). The apparent molecular weights of the migrated fragments are shown in thousands.

mice (~140 days of age) did not display PrP 22-24 (Fig. 3D). A shorter PrP fragment of ~19 kDa was detected using the cold PK assay in all mice when blots were stained with anti-PrP RO73 polyclonal antiserum (Fig. 3D) but not when using the 5449 antiserum, which reacts only with residues 89 to 143 of MoPrP(P101L) (Fig. 3E and F). The 19-kDa fragment probably corresponds to the C-terminal portion of PrP.

Transmission of mouse GSS(P101L) prions. We measured prion infectivity in the brains of uninoculated Tg2866 mice after they spontaneously developed CNS dysfunction at ~130 days of age. Brain homogenates from Tg2866 mice were subjected to PTA precipitation alone or in combination with PK digestion before bioassay in Tg196 mice (Table 3). Untreated brain homogenates from Tg2866 mice produced disease in Tg196 mice at ~305 days, while PTA precipitation followed by PK digestion reduced the incubation time to ~225 days. This ~80-day reduction in the incubation time is highly significant, with a P value of <0.0014 (analysis of variance), arguing that the prions in the brains of Tg2866 mice are resistant to PK digestion.

Similar results were obtained when brain extracts were prepared from Tg196 mice previously inoculated with Tg2866 brain homogenates. The untreated homogenates from the Tg196(2866) mice produced disease in inoculated Tg196 mice after ~350 days, while PTA precipitation followed by PK digestion reduced the incubation time to ~280 days (Table 3). This ~70-day reduction in the incubation time is highly significant, with a P value of < 0.0005 (analysis of variance), arguing that the prions in the brains of Tg196(2866) mice are also resistant to PK digestion.

In contrast to the studies with inocula derived from the brains of Tg2866 mice, untreated inocula from the brains of neurologically normal Tg196 mice at ~300 days of age produced disease in six of seven Tg196 mice after ~480 days (Table 3). Moreover, inocula subjected to PTA precipitation followed by PK digestion produced disease at ~480 days but only in one of nine Tg196 mice. When 301V prions were inoculated into Tg196 mice, the incubation period was ~145 days, which was reduced by ~15 days when the inoculum was first subjected to PTA precipitation and PK digestion; this 10% reduction in incubation time is statistically insignificant. The 301V prions were initially isolated from BSE brain by passage in VM mice harboring the $Prnp^{b/b}$ alleles and subsequently passaged in B6.1 mice also carrying $Prnp^{b/b}$ alleles, with an incubation time of ~115 days (Table 2). On subsequent passages in Tg196 mice, the incubation times ranged from 115 to 145 days (Tables 2 and 3).

Age-dependent accumulation of prions in Tg2866 mice. We measured prion infectivity in the brains of Tg2866 mice by sacrificing the mice at various ages and inoculating their brain extracts into Tg196 mice. BH from Tg2866 mice sacrificed either at birth or at 56 days of age contained no detectable levels of prion infectivity, based on bioassays in Tg196 mice (Fig. 4E). Low levels of infectivity were found in 84-day-old Tg2866 mice: brain extracts from these mice inoculated into Tg196 mice induced disease in two of nine animals at ~440 days postinoculation (Fig. 4E). Brain extracts from 112-day-old Tg2866 mice produced disease after ~350 days of incubation in 9 of 10 animals. When Tg2866 mice developed signs of CNS dysfunction at ~130 days, the mice were sacrificed and their BH were inoculated into Tg196 mice. All eight inoculated Tg196 mice developed disease, with a mean incubation period of ~260 days (Fig. 4E). No infectivity was detected in the brains of age-matched, control Tg4053 mice (130 days of age), based on bioassays in Tg196 mice (0 of 10 animals, >500 days); Tg4053 mice express wt MoPrP at levels similar to mutant MoPrP(P101L) expressed in Tg2866 mice. This progressive shortening of incubation periods is consistent with an increase in the titer of infectious prions in the brains of Tg2866 mice as they age.

The progressive accumulation of infectious GSS(P101L) prions in Tg2866 mice as they aged correlated with the appearance of $sPrP^{Sc}$(P101L). PrP 22-24 was detected at 112 days and ~130 days using the cold PK digestion protocol (Fig. 4C). Curiously, Tg2866 mice showed a transient postnatal upregulation of mutant MoPrP(P101L) expression between 14 and 56 days of age (Fig. 4A). Levels of $sPrP^{Sc}$(P101L) were highest in

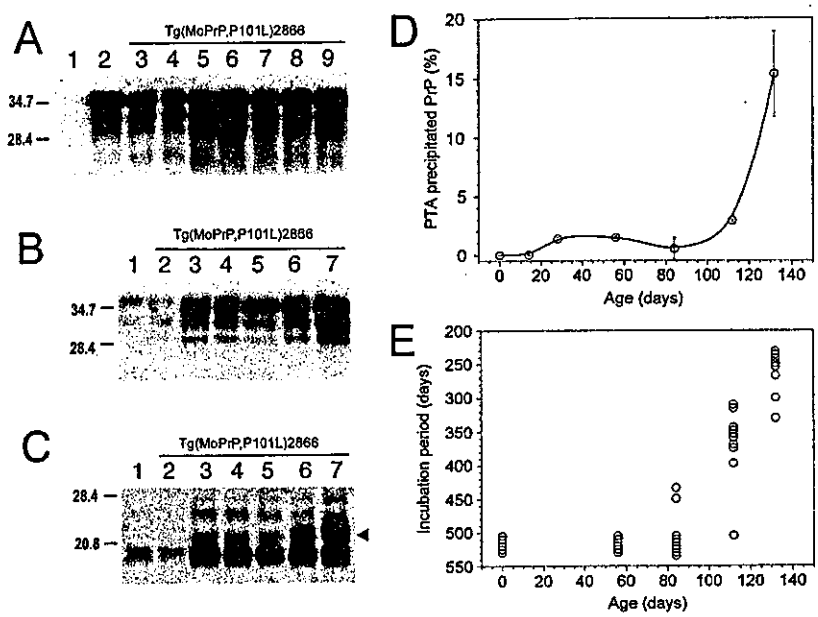

FIG. 4. Progressive accumulation of abnormal MoPrP(P101L) conformers (A to D) correlates with the accumulation of infectious prions (E) as a function of age in Tg(MoPrP,P101L)2866/$Prnp^{0/0}$ mice. Presymptomatic animals were sacrificed at birth, at 14 days, 28 days, 56 days, 84 days, or 112 days of age or at ~132 days (when diagnosed with CNS dysfunction). Blots were developed using the RO73 polyclonal antibody. The apparent molecular weights of the migrated fragments are shown in thousands. (A) Untreated brain homogenates from $Prnp^{0/0}$ mice (lane 1), Tg4053 mice (lane 2), or Tg2866 mice (lanes 3 to 9) sacrificed at birth (lane 3), 14 days (lane 4), 28 days (lane 5), 56 days (lane 6), 84 days (lane 7), 112 days (lane 8), or ~132 days (lane 9). (B) Brain homogenates from Tg4053 mice (lane 1), Tg2866 mice sacrificed at 14 days (lane 2), 28 days (lane 3), 56 days (lane 4), 84 days (lane 5), 112 days (lane 6), or ~132 days (lane 7). Samples were precipitated with PTA prior to immunoblotting. (C) Brain homogenates subjected to cold PK digestion followed by PTA precipitation. Lane assignments are as described for panel B. The presence of a 22-kDa to 24-kDa PrP fragment specific to infectious GSS prions is indicated by the arrowhead. (D) The accumulation of abnormal PrP conformers in the brains of aging Tg(MoPrP,P101L)2866/$Prnp^{0/0}$ mice was quantified using the CDI with the RO73 antiserum and a secondary Eu-labeled anti-rabbit polyclonal antibody. (E) The same brain homogenates from aging Tg(MoPrP,P101L)2866/$Prnp^{0/0}$ mice used in the CDI were inoculated into Tg(MoPrP,P101L)196/$Prnp^{0/0}$ mice to measure incubation times, which are inversely proportional to the prion titer (38). Animals that did not display signs of neurological dysfunction were sacrificed after 500 days.

Tg2866 mice at ~130 days of age, when these mice developed CNS disease (Fig. 4B).

GSS(P102L) prions in human patients and Tg mice. We assessed whether the progressive accumulation of abnormal PrP conformers observed in Tg2866 mice applies to GSS patients and to Tg mice expressing the MHu2M transgene with the corresponding P102L mutation, designated Tg(MHu2M,P102L)69/$Prnp^{0/0}$ mice. Tg69 mice developed CNS disease spontaneously at ~400 days of age; however, when Tg69 mice were inoculated with brain extracts from patients who died of GSS, they developed disease ~170 days after inoculation.

Brain samples from Tg69 mice and from patients with GSS were subjected to PTA precipitation alone or after cold PK digestion. These brain samples displayed increased levels of $sHuPrP^{Sc}$(P102L) compared to untreated samples (Fig. 5A, B, and D). Mutant HuPrP 22-24 was found in Tg69 mice at 200 days of age (Fig. 5D) and at much higher levels in spontaneously ill Tg69 mice at ~360 days of age (Fig. 5F and H).

Conformation-dependent immunoassay. The development of the CDI permitted measurement of both $rPrP^{Sc}$ and $sPrP^{Sc}$ (39). We used the CDI to measure the relative ratios of $rPrP^{Sc}$ and $sPrP^{Sc}$ in the brains of Tg196 and Tg2866 mice (Table 1). No $sPrP^{Sc}$(P101L) was detectable in the brains of uninoculated Tg196 mice, while $sPrP^{Sc}$(P101L) comprised ~15% of total PrP in spontaneously ill Tg2866 mice (Fig. 6A). As noted above, $sPrP^{Sc}$(P101L) is measured by cold PK digestion followed by PTA precipitation. In the brains of Tg196 mice inoculated with prions from Tg2866 mice, $sPrP^{Sc}$(P101L) accounted for ~20% of total PrP. In the brains of Tg196 mice inoculated with prions derived from sheep (RML) or cattle (301V), $sPrP^{Sc}$(P101L) comprised ~25% of total PrP. PK digestion followed by ultracentrifugation showed that $rPrP^{Sc}$ (P101L) was undetectable in the brains of uninoculated Tg196 mice. In contrast, $rPrP^{Sc}$(P101L) represented ~5% of the total PrP in the brains of spontaneously ill Tg2866 mice (Fig. 6A). In Tg196 mice inoculated with prions from Tg2866 mice, ~10% of total PrP was PK resistant; in Tg196 mice inoculated with either RML or 301V prions, ~20% of the total PrP was PK resistant.

When $rPrP^{Sc}$(P101L) was plotted as a function of the ratio of denatured (D) to native (N) PrP^{Sc}, as measured by time-resolved fluorescence spectrometry (Fig. 6B), the PrP^{Sc} (P101L) conformers found in the brains of spontaneously ill Tg2866 mice were distinct from those found in Tg196 mice inoculated with RML or 301V prions. The PrP^{Sc}(P101L) conformers found in spontaneously ill Tg2866 mice were indistinguishable from those found in the three groups of mice: (i) Tg196 mice inoculated with the MoPrP(89-143,P101L) peptide; (ii) Tg196 mice inoculated with brain extracts from ill Tg196 mice that were inoculated with the MoPrP(89-143, P101L) peptide; and (iii) Tg196 inoculated with brain extracts

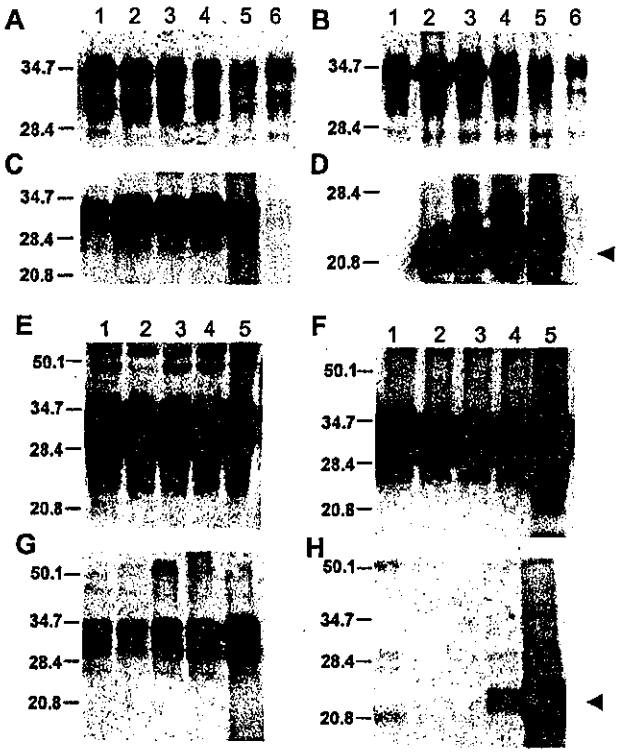

FIG. 5. Aberrant HuPrP(P102L) conformers present in the brains of GSS patients and GSS-inoculated Tg mice (A to D) are indistinguishable from those that progressively accumulate in spontaneously ill chimeric Tg(MHu2M,P102L) mice (E to H). Samples were developed using the 3F4 monoclonal antibody. The apparent molecular weights of migrated fragments are shown in thousands. The presence of a 22-kDa to 24-kDa PrP fragment specific to GSS prions is indicated by the arrowheads. (A to D) Brain homogenates from spontaneously ill Tg(MHu2M,P102L)69/$Prnp^{0/0}$ mice (lane 2), Tg(MHu2M,P102L) mice inoculated with homogenates from GSS patients expressing either Val (lane 3) or Met (lane 4) at codon 129, and a GSS(P102L,M129) patient (lane 5). As controls, homogenates from an age-matched, healthy Tg(MHu2M)$Prnp^{0/0}$ mouse (lane 1) and normal human brain (lane 6) are shown. (E to H) Brain homogenates from spontaneously ill Tg69 mice sacrificed at 50 days (lane 2), 100 days (lane 3), 200 days (lane 4), ~360 days (lane 5), when the mice became ill, demonstrate the accumulation of PrP^{Sc} conformers that are similar to those observed in GSS patients. As a control, homogenate from a healthy, age-matched Tg(MHu2M)$Prnp^{0/0}$ mouse (lane 1) is shown. Samples were untreated (A and E), precipitated with PTA (B and F), digested with PK followed by ultracentrifugation (C and G), or subjected to cold PK digestion followed by PTA precipitation (D and H).

from ill Tg2866 mice. These findings support the contention that the GSS prions either arising spontaneously in Tg2866 mice or induced in Tg196 mice by the 55-mer MoPrP(89-143, P101L) peptide are distinct from prion strains derived from sheep with scrapie (RML) and cattle with BSE (301V).

DISCUSSION

The results reported here permit, for the first time, biophysical correlations with prion infectivity generated in mice expressing MoPrP(P101L) transgenes. Although the first Tg mice expressing MoPrP(P101L) were constructed more than a decade ago (26, 27, 47), the lack of biophysically detectable alterations in mutant MoPrP(P101L) has compromised the utility of this model system, until now. Selective precipitation of PrP^{Sc}(P101L) with PTA in combination with cold PK digestion provides a new tool for dissecting the molecular mechanisms of inherited prion diseases. In addition, the results presented here coupled with an earlier report (29) argue that MoPrP(89-143, P101L) in a β-rich conformation triggers the generation of de novo GSS prions; indeed, our findings provide compelling evidence that this 55-mer mutant peptide folded into a β-rich structure is a synthetic prion.

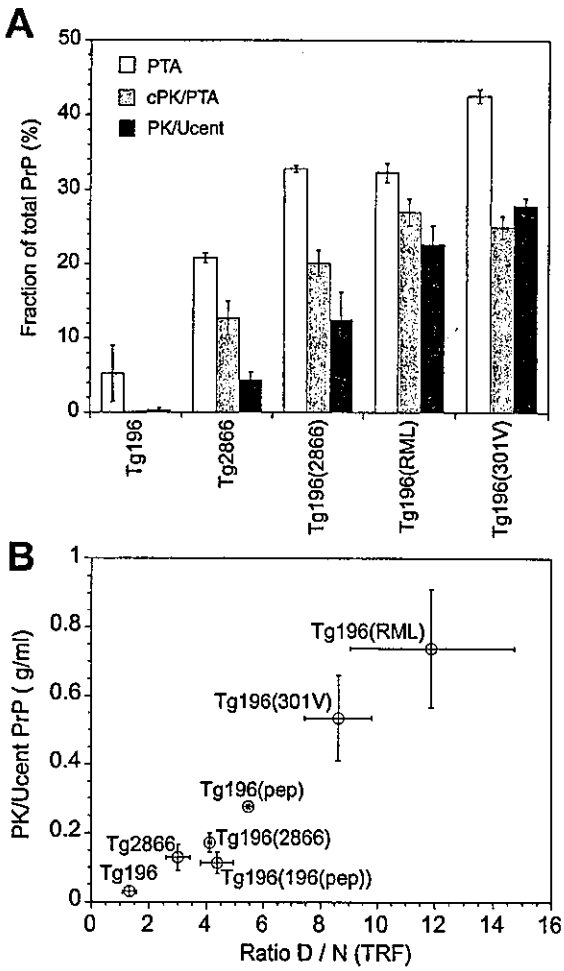

FIG. 6. Differential proteolytic resistance of aberrant, distinct PrP conformers in the brains of Tg(MoPrP,P101L) mice detected by the CDI. (A) Brain homogenates from spontaneously ill Tg(MoPrP, P101L)2866/$Prnp^{0/0}$ mice and Tg(MoPrP,P101L)196/$Prnp^{0/0}$ mice inoculated with RML prions, 301V prions, or GSS(P101L) prions from ill Tg2866 mice. Controls were age matched, uninoculated Tg mice. Samples were either left untreated (total PrP content), PTA precipitated, digested with cold PK followed by PTA precipitation (cPK/PTA), or digested with PK followed by ultracentrifugation (PK/Ucent). Results are shown as the fraction of total PrP recovered after each treatment. (B) Amount of $rPrP^{Sc}$ recovered after ultracentrifugation plotted as a function of the amount of antibody bound to the denatured and native forms of PrP (D:N ratio). Samples were obtained from the same mice depicted in panel A, in addition to Tg(MoPrP,P101L)196/$Prnp^{0/0}$ mice inoculated with the β-rich MoPrP(89-143,P101L) peptide on first [Tg196(pep)] and second [Tg196(196(pep))] passage. Data points and bars represent the means ± standard errors of the mean obtained from three independent measurements.

Synthetic prions. In an effort to construct a synthetic prion, we chose to focus our efforts on a genetic form of prion disease in order to bias the folding of PrP into a PrP^{Sc} isoform. Multiple attempts to generate prion infectivity from refolded recombinant PrPs have been unsuccessful to date (5–7). Since GSS(P102L) is the only inherited prion disease that has been successfully modeled in mice with respect to generating infectivity de novo, we chose to exploit the P102L mutation. To produce a synthetic prion, we constructed the 55-mer MoPrP (89-143,P101L) peptide using solid-phase peptide synthesis. When folded into a β-rich conformation, MoPrP(89-143, P101L) induced prion disease in Tg196 mice (Table 2) (29). The same peptide did not induce disease when it was not folded into a β-rich conformation. That the peptide must be in β-rich structure and the host must express MoPrP(P101L) in order to induce disease underscores the conformational specificity of prion propagation.

We report here that the disease induced in Tg196 mice by the β-rich MoPrP(89-143,P101L) peptide can be serially transmitted to Tg196 mice with an incubation time of ~350 days (Table 2). The presence of large multicentric plaques, which deposit in the neocortex, caudate nucleus, corpus callosum, hippocampus, and cerebellar cortex, together with focal vacuolar changes, corroborate the distinct characteristics of these GSS prions. From these experimental findings and those presented previously, we argue that the mutant 55-mer, β-rich peptide fulfills all of the criteria required for designation as a synthetic prion.

The neuropathologic changes characteristic of humans carrying the GSS(P102L) mutation, including large, multicentric plaques that stain with anti-PrP antibodies, are preserved in Tg(MoPrP,P101L) mice that develop prion disease spontaneously as well as in those that develop disease after inoculation with GSS prions or with the mutant 55-mer β-rich peptide. In contrast, when human GSS(P102L) prions are transmitted to nonhuman primates or non-Tg mice, these GSS-type plaques are rarely found (1, 32, 46). This distinction argues that the P→L substitution imposes a conformational constraint on host PrP^{C} that is required to preserve the disease characteristics of GSS.

It is noteworthy that polypeptides comprising the N domain of the yeast Sup35 protein have been expressed in *Escherichia coli* and folded into a β-rich conformation (3, 44). Such polypeptides readily polymerize into amyloid, which has been transferred into [PSI^{-}] *Saccharomyces cerevisiae* that in turn becomes [*PSI*$^{+}$], the prion state. As with the mutant 55-mer, β-rich peptide studies reported previously (29), these experiments with yeast argue for the production of a synthetic prion and contend that prions are composed only of protein, in accord with a wealth of other data (36).

Prion strains. Based on differences in resistance to limited proteolysis, two groups of prion strains can be distinguished: (i) those with low levels and (ii) those with high levels of $rPrP^{Sc}$ (P101L). Strains with low levels of $rPrP^{Sc}$(P101L) are formed spontaneously in Tg2866 mice and are formed in Tg196 mice after inoculation with either GSS(P101L) prions or the mutant 55-mer β-rich synthetic peptide. Prion strains with high levels of $rPrP^{Sc}$(P101L) were formed in Tg196 mice after inoculation with RML, 139A, or 301V prions. This last group of prion strains can be subdivided into two groups based on their incubation times in Tg196 mice: RML and 139A prions produce long incubation times, whereas 301V prions result in short incubation times. The P101L substitution in Tg196 mice introduced a transmission barrier and lengthened the incubation periods of RML and 139A prions (~180 days) compared to those observed in wt *Prnp*$^{a/a}$ mice (~130 days). In contrast, the replication of 301V prions in Tg196 mice did not encounter a transmission barrier, with incubation periods of ~125 days, similar to those found in *Prnp*$^{b/b}$ B6.I mice (Tables 2 and 3) (12). Since the phenomenon of transmission barriers induced by mutations was observed also in yeast prion [*PSI*$^{+}$], the mechanism appears to be a general paradigm for all prions regardless of the host or strain (17).

Conformational characteristics of PrP^{Sc}. The wide use of limited proteolysis to detect PrP 27-30 created the expectation that Tg(MoPrP,P101L) mice spontaneously developing CNS disease should possess readily detectable levels of mutant PrP 27-30 (15, 16). When PrP 27-30 was not found after limited PK digestion at 37°C, the modeling of GSS in Tg mice was thought to be unconvincing and prompted some investigators to doubt the interpretation of genetic linkage studies of humans carrying pathological mutations in the PrP gene.

In the studies reported here, we demonstrate that PrP^{Sc} conformers accumulate in the brains of Tg(MoPrP,P101L) mice that develop prion disease spontaneously as well as those that were inoculated with either GSS prions or the mutant 55-mer β-rich peptide. By modifying the conditions for limited proteolysis, we consistently demonstrated high levels of a disease-specific $sPrP^{Sc}$(P101L) conformer that generated PrP 22-24 upon cold PK digestion that was absent from the brains of wt mice (Table 1). Moreover, $sPrP^{Sc}$(P101L) accumulated in the brains of Tg2866 mice as a function of age and reached maximal levels when the mice displayed neurologic signs of prion disease (Fig. 5).

In the studies described here, PrP^{Sc}(P101L) adopted one conformation that was most readily detectable only after cold PK digestion and another conformation that was assayed by PK digestion at 37°C. Cold PK digestion demonstrated the presence of $sPrP^{Sc}$(P101L) in the brains of Tg2866 mice that develop prion disease spontaneously as well as of Tg196 mice that were inoculated with either GSS prions or the mutant 55-mer β-rich peptide (Fig. 3 to 5). PK digestion at 37°C was used to demonstrate $rPrP^{Sc}$(P101L) in the brains of Tg196 mice inoculated with prion strains derived from sheep with scrapie (RML and 139A prions) or cattle with BSE (301V prions) (Fig. 3C).

Defining the conformations of PrP^{Sc}(P101L) and wt PrP^{Sc} molecules promises to be difficult, since both are quite insoluble. Currently, the best approach to elucidating the structural features of wt PrP^{Sc} has been by electron crystallography of two-dimensional crystals (50). From the PK digestion studies of RML, 139A, and 301V prions propagated in Tg196 mice, it is reasonable to argue that $rPrP^{Sc}$(P101L) and wt $rPrP^{Sc}$ probably have similar structures. It is less clear how $sPrP^{Sc}$(P101L) in the brains of ill Tg2866 and Tg196 mice is related to wt $sPrP^{Sc}$. Assessing this relationship is difficult because no procedure has been developed to separate wt $sPrP^{Sc}$ from wt $rPrP^{Sc}$. Using the CDI, wt $sPrP^{Sc}$ can be calculated by subtracting PrP 27-30 from total PrP^{Sc}.

When the brains of Tg2866 mice were subjected to PK

digestion before or after PTA precipitation and inoculated into mice, the resulting incubation times were shorter than those obtained with untreated brain homogenates (Table 3), presumably reflecting increased titers due to the concentration of prions by selective PTA precipitation. Moreover, these results indicate that prion infectivity in the brains of Tg2866 mice is resistant to limited digestion with 25 μg of PK/ml for 1 h at 37°C. Similar resistance to proteolytic digestion was observed in the brains of Tg196 mice inoculated with either Tg2866 brain homogenates or 301V prions. The characteristics of different PrP isoforms are summarized in Table 1.

Mechanisms of neurodegeneration. Although there are many examples of modified PrP^C molecules, only PrP(P101L) has been shown to initiate an experimental prion disease that is transmissible. In studies using Tg mice, the expression of the D178N mutation did not produce neurologic deficits. The E200K and A117V mutations produced neurologic diseases, but brains from Tg mice carrying these mutations failed to transmit disease on passage in wt or isogenic hosts (24; P. Tremblay et al., unpublished observations). Similarly, the expression of a PrP transgene harboring an octapeptide repeat expansion from 5 to 14 repeats has been shown to initiate a spontaneous neurodegenerative condition similar to that observed in humans with prion disease (18, 19), but despite the accumulation of insoluble PrP conformers displaying low levels of protease resistance, the transmissibility of this disease has yet to be demonstrated. Expression of various designer mutations that led to the generation of PrP^C molecules with a transmembrane topology produced neurologic deficits correlating to the synthesis of topologically distinct, transmembrane PrP molecules (24, 25); again, attempts to transmit these diseases have failed (R. S. Hegde et al., unpublished observations). The general model emerging from all those experiments suggests that there are two probably independent misfolding pathways of mutant PrP: one leading to accumulation of misfolded conformers causing neurodegeneration and the other pathway leading to the accumulation of conformers that are infectious; whether the infectious conformers are also those that cause neurodegeneration remains to be established.

New directions in prion research. The discoveries reported here describe relatively crude biophysical correlations with prion infectivity generated in mice expressing MoPrP(P101L) transgenes. More detailed analyses might prove to be relevant in dissecting the mechanism of prion formation in the inherited prion diseases. The MoPrP(P101L) transgene has been unexpectedly useful in the study of prion strains. Coupled with new approaches using PTA precipitation and cold PK digestion, Tg mice expressing MoPrP(P101L) may increase our understanding of the mechanism by which prions are formed spontaneously as well as the structural features that encipher strain-specific information.

ACKNOWLEDGMENTS

This work was supported by grants from the National Institutes of Health (AG02132 and AG010770) and by a gift from the Leila Y. and G. Harold Mathers Charitable Foundation.

We thank the Hunter's Point Animal Facility.

REFERENCES

1. **Baker, H. F., L. W. Duchen, J. M. Jacobs, and R. M. Ridley.** 1990. Spongiform encephalopathy transmitted experimentally from Creutzfeldt-Jakob and familial Gerstmann-Sträussler-Scheinker diseases. Brain 113:1891–1909.
2. **Baker, H. F., R. M. Ridley, and T. J. Crow.** 1985. Experimental transmission of an autosomal dominant spongiform encephalopathy: does the infectious agent originate in the human genome? Br. Med. J. 291:299–302.
3. **Balbirnie, M., R. Grothe, and D. S. Eisenberg.** 2001. An amyloid-forming peptide from the yeast prion Sup35 reveals a dehydrated β-sheet structure for amyloid. Proc. Natl. Acad. Sci. USA 98:2375–2380.
4. **Barry, R. A., and S. B. Prusiner.** 1986. Monoclonal antibodies to the cellular and scrapie prion proteins. J. Infect. Dis. 154:518–521.
5. **Baskakov, I. V., C. Aagaard, I. Mehlhorn, H. Wille, D. Groth, M. A. Baldwin, S. B. Prusiner, and F. E. Cohen.** 2000. Self-assembly of recombinant prion protein of 106 residues. Biochemistry 39:2792–2804.
6. **Baskakov, I. V., G. Legname, M. A. Baldwin, S. B. Prusiner, and F. E. Cohen.** 2002. Pathway complexity of prion protein assembly into amyloid. J. Biol. Chem. 277:21140–21148.
7. **Baskakov, I. V., G. Legname, S. B. Prusiner, and F. E. Cohen.** 2001. Folding of prion protein to its native α-helical conformation is under kinetic control. J. Biol. Chem. 276:19687–19690.
8. **Bolton, D. C., M. P. McKinley, and S. B. Prusiner.** 1982. Identification of a protein that purifies with the scrapie prion. Science 218:1309–1311.
9. **Brown, P., C. J. Gibbs, Jr., P. Rodgers-Johnson, D. M. Asher, M. P. Sulima, A. Bacote, L. G. Goldfarb, and D. C. Gajdusek.** 1994. Human spongiform encephalopathy: the National Institutes of Health series of 300 cases of experimentally transmitted disease. Ann. Neurol. 35:513–529.
10. **Bruce, M., A. Chree, I. McConnell, J. Foster, G. Pearson, and H. Fraser.** 1994. Transmission of bovine spongiform encephalopathy and scrapie to mice: strain variation and the species barrier. Phil. Trans. R. Soc. Lond. B 343:405–411.
11. **Büeler, H., M. Fisher, Y. Lang, H. Bluethmann, H.-P. Lipp, S. J. DeArmond, S. B. Prusiner, M. Aguet, and C. Weissmann.** 1992. Normal development and behaviour of mice lacking the neuronal cell-surface PrP protein. Nature 356:577–582.
12. **Carlson, G. A., C. Ebeling, S.-L. Yang, G. Telling, M. Torchia, D. Groth, D. Westaway, S. J. DeArmond, and S. B. Prusiner.** 1994. Prion isolate specified allotypic interactions between the cellular and scrapie prion proteins in congenic and transgenic mice. Proc. Natl. Acad. Sci. USA 91:5690–5694.
13. **Carlson, G. A., D. T. Kingsbury, P. A. Goodman, S. Coleman, S. T. Marshall, S. DeArmond, D. Westaway, and S. B. Prusiner.** 1986. Linkage of prion protein and scrapie incubation time genes. Cell 46:503–511.
14. **Chandler, R. L.** 1961. Encephalopathy in mice produced by inoculation with scrapie brain material. Lancet i:1378–1379.
15. **Chesebro, B.** 1998. Prion diseases: BSE and prions: uncertainties about the agent. Science 279:42–43.
16. **Chesebro, B.** 1992. PrP and the scrapie agent. Nature 356:560.
17. **Chien, P., A. H. DePace, S. R. Collins, and J. S. Weissman.** 2003. Generation of prion transmission barriers by mutational control of amyloid conformations. Nature 424:948–951.
18. **Chiesa, R., B. Drisaldi, E. Quaglio, A. Migheli, P. Piccardo, B. Ghetti, and D. A. Harris.** 2000. Accumulation of protease-resistant prion protein (PrP) and apoptosis of cerebellar granule cells in transgenic mice expressing a PrP insertional mutation. Proc. Natl. Acad. Sci. USA 97:5574–5579.
19. **Chiesa, R., P. Piccardo, B. Ghetti, and D. A. Harris.** 1998. Neurological illness in transgenic mice expressing a prion protein with an insertional mutation. Neuron 21:1339–1351.
20. **DeArmond, S. J., and J. W. Ironside.** 1999. Neuropathology of prion diseases, p. 585–652. *In* S. B. Prusiner (ed.), Prion biology and diseases. Cold Spring Harbor Laboratory Press, Cold Spring Harbor, N.Y.
21. **Dickinson, A. G.** 1976. Scrapie in sheep and goats, p. 209–241. *In* R. H. Kimberlin (ed.), Slow virus diseases of animals and man. North-Holland Publishing, Amsterdam, The Netherlands.
22. **Fraser, H., M. E. Bruce, A. Chree, I. McConnell, and G. A. H. Wells.** 1992. Transmission of bovine spongiform encephalopathy and scrapie to mice. J. Gen. Virol. 73:1891–1897.
23. **Gambetti, P., R. B. Peterson, P. Parchi, S. G. Chen, S. Capellari, L. Goldfarb, R. Gabizon, P. Montagna, E. Lugaresi, P. Piccardo, and B. Ghetti.** 1999. Inherited prion diseases, p. 509–583. *In* S. B. Prusiner (ed.), Prion biology and diseases. Cold Spring Harbor Laboratory Press, Cold Spring Harbor, N.Y.
24. **Hegde, R. S., J. A. Mastrianni, M. R. Scott, K. A. DeFea, P. Tremblay, M. Torchia, S. J. DeArmond, S. B. Prusiner, and V. R. Lingappa.** 1998. A transmembrane form of the prion protein in neurodegenerative disease. Science 279:827–834.
25. **Hegde, R. S., P. Tremblay, D. Groth, S. B. Prusiner, and V. R. Lingappa.** 1999. Transmissible and genetic prion diseases share a common pathway of neurodegeneration. Nature 402:822–826.
26. **Hsiao, K., M. Scott, D. Foster, S. J. DeArmond, and S. B. Prusiner.** 1990. Towards a model of Gerstmann-Sträussler-Scheinker syndrome in transgenic mice. Soc. Neurosci. Abstr. 16(part 2):1138.
27. **Hsiao, K. K., D. Groth, M. Scott, S.-L. Yang, H. Serban, D. Rapp, D. Foster, M. Torchia, S. J. DeArmond, and S. B. Prusiner.** 1994. Serial transmission in rodents of neurodegeneration from transgenic mice expressing mutant prion protein. Proc. Natl. Acad. Sci. USA 91:9126–9130.
28. **Hsiao, K. K., M. Scott, D. Foster, D. F. Groth, S. J. DeArmond, and S. B.**

Prusiner. 1990. Spontaneous neurodegeneration in transgenic mice with mutant prion protein. Science 250:1587–1590.
29. Kaneko, K., H. L. Ball, H. Wille, H. Zhang, D. Groth, M. Torchia, P. Tremblay, J. Safar, S. B. Prusiner, S. J. DeArmond, M. A. Baldwin, and F. E. Cohen. 2000. A synthetic peptide initiates Gerstmann-Sträussler-Scheinker (GSS) disease in transgenic mice. J. Mol. Biol. 295:997–1007.
30. Kascsak, R. J., R. Rubenstein, P. A. Merz, M. Tonna-DeMasi, R. Fersko, R. I. Carp, H. M. Wisniewski, and H. Diringer. 1987. Mouse polyclonal and monoclonal antibody to scrapie-associated fibril proteins. J. Virol. 61:3688–3693.
31. Manson, J. C., E. Jameison, H. Baybutt, N. L. Tuzi, R. Barron, I. McConnell, R. Somerville, J. Ironside, R. Will, M.-S. Sy, D. W. Melton, J. Hope, and C. Bostock. 1999. A single aminò acid alteration (101L) introduced into murine PrP dramatically alters incubation time of transmissible spongiform encephalopathy. EMBO J. 18:6855–6864.
32. Masters, C. L., D. C. Gajdusek, and C. J. Gibbs, Jr. 1981. Creutzfeldt-Jakob disease virus isolations from the Gerstmann-Sträussler syndrome. Brain 104: 559–588.
33. Moore, R. C., J. Hope, P. A. McBride, I. McConnell, J. Selfridge, D. W. Melton, and J. C. Manson. 1998. Mice with gene targetted prion protein alterations show that *Prnp*, Sinc and *Prni* are congruent. Nat. Genet. 18:118–125.
34. Muramoto, T., S. J. DeArmond, M. Scott, G. C. Telling, F. E. Cohen, and S. B. Prusiner. 1997. Heritable disorder resembling neuronal storage disease in mice expressing prion protein with deletion of an α-helix. Nat. Med. 3:750–755.
35. Peretz, D., R. A. Williamson, Y. Matsunaga, H. Serban, C. Pinilla, R. B. Bastidas, R. Rozenshteyn, T. L. James, R. A. Houghten, F. E. Cohen, S. B. Prusiner, and D. R. Burton. 1997. A conformational transition at the N-terminus of the prion protein features in formation of the scrapie isoform. J. Mol. Biol. 273:614–622.
36. Prusiner, S. B. 1998. Prions. Proc. Natl. Acad. Sci. USA 95:13363–13383.
37. Prusiner, S. B., D. C. Bolton, D. F. Groth, K. A. Bowman, S. P. Cochran, and M. P. McKinley. 1982. Further purification and characterization of scrapie prions. Biochemistry 21:6942–6950.
38. Prusiner, S. B., S. P. Cochran, D. F. Groth, D. E. Downey, K. A. Bowman, and H. M. Martinez. 1982. Measurement of the scrapie agent using an incubation time interval assay. Ann. Neurol. 11:353–358.
39. Safar, J., H. Wille, V. Itri, D. Groth, H. Serban, M. Torchia, F. E. Cohen, and S. B. Prusiner. 1998. Eight prion strains have PrP^{Sc} molecules with different conformations. Nat. Med. 4:1157–1165.
40. Safar, J. G., M. Scott, J. Monaghan, C. Deering, S. Didorenko, J. Vergara, H. Ball, G. Legname, E. Leclerc, L. Solforosi, H. Serban, D. Groth, D. R. Burton, S. B. Prusiner, and R. A. Williamson. 2002. Measuring prions causing bovine spongiform encephalopathy or chronic wasting disease by immunoassays and transgenic mice. Nat. Biotechnol. 20:1147–1150.
41. Scott, M., D. Foster, C. Mirenda, D. Serban, F. Coufal, M. Wälchli, M. Torchia, D. Groth, G. Carlson, S. J. DeArmond, D. Westaway, and S. B. Prusiner. 1989. Transgenic mice expressing hamster prion protein produce species-specific scrapie infectivity and amyloid plaques. Cell 59:847–857.
42. Scott, M. R., R. Will, J. Ironside, H.-O. B. Nguyen, P. Tremblay, S. J. DeArmond, and S. B. Prusiner. 1999. Compelling transgenetic evidence for transmission of bovine spongiform encephalopathy prions to humans. Proc. Natl. Acad. Sci. USA 96:15137–15142.
43. Serban, D., A. Taraboulos, S. J. DeArmond, and S. B. Prusiner. 1990. Rapid detection of Creutzfeldt-Jakob disease and scrapie prion proteins. Neurology 40:110–117.
44. Sparrer, H. E., A. Santoso, F. C. Szoka, Jr., and J. S. Weissman. 2000. Evidence for the prion hypothesis: induction of the yeast [*PSI*$^+$] factor by in vitro-converted Sup35 protein. Science 289:595–599.
45. Taraboulos, A., K. Jendroska, D. Serban, S.-L. Yang, S. J. DeArmond, and S. B. Prusiner. 1992. Regional mapping of prion proteins in brains. Proc. Natl. Acad. Sci. USA 89:7620–7624.
46. Tateishi, J., T. Kitamoto, M. Z. Hoque, and H. Furukawa. 1996. Experimental transmission of Creutzfeldt-Jakob disease and related diseases to rodents. Neurology 46:532–537.
47. Telling, G. C., T. Haga, M. Torchia, P. Tremblay, S. J. DeArmond, and S. B. Prusiner. 1996. Interactions between wild-type and mutant prion proteins modulate neurodegeneration in transgenic mice. Genes Dev. 10:1736–1750.
48. Telling, G. C., M. Scott, J. Mastrianni, R. Gabizon, M. Torchia, F. E. Cohen, S. J. DeArmond, and S. B. Prusiner. 1995. Prion propagation in mice expressing human and chimeric PrP transgenes implicates the interaction of cellular PrP with another protein. Cell 83:79–90.
49. Westaway, D., P. A. Goodman, C. A. Mirenda, M. P. McKinley, G. A. Carlson, and S. B. Prusiner. 1987. Distinct prion proteins in short and long scrapie incubation period mice. Cell 51:651–662.
50. Wille, H., M. D. Michelitsch, V. Guénebaut, S. Supattapone, A. Serban, F. E. Cohen, D. A. Agard, and S. B. Prusiner. 2002. Structural studies of the scrapie prion protein by electron crystallography. Proc. Natl. Acad. Sci. USA 99:3563–3568.

Available online at www.sciencedirect.com
SCIENCE DIRECT®
Biochemical and Biophysical Research Communications 315 (2004) 802–807
BBRC
www.elsevier.com/locate/ybbrc

Anterograde and retrograde intracellular trafficking of fluorescent cellular prion protein

Naomi S. Hachiya, Kota Watanabe, Makiko Yamada, Yuji Sakasegawa, and Kiyotoshi Kaneko*

Department of Cortical Function Disorders, National Institute of Neuroscience (NIN), National Center of Neurology and Psychiatry (NCNP), and Core Research for Evolutional Science and Technology (CREST), Japan Science and Technology Agency, Tokyo 187-8502, Japan

Received 22 January 2004

Abstract

In order to investigate the microtubule-associated intracellular trafficking of the NH2-terminal cellular prion protein (PrP^C) fragment [Biochem. Biophys. Res. Commun. 313 (2004) 818], we performed a real-time imaging of fluorescent PrP^C (GFP-PrP^C) in living cells. Such GFP-PrP^C exhibited an anterograde movement towards the direction of plasma membranes at a speed of 140–180 nm/s, and a retrograde movement inwardly at a speed of 1.0–1.2 μm/s. The anterograde and retrograde movements of GFP-PrP^C were blocked by a kinesin family inhibitor (AMP-PNP) and a dynein family inhibitor (vanadate), respectively. Furthermore, anti-kinesin antibody (α-kinesin) blocked its anterograde motility, whereas anti-dynein antibody (α-dynein) blocked its retrograde motility. These data suggested the kinesin family-driven anterograde and the dynein-driven retrograde movements of GFP-PrP^C. Mapping of the interacting domains of PrP^C identified amino acid residues indispensable for interactions with kinesin family: NH2-terminal mouse (Mo) residues 53–91 and dynein: NH2-terminal Mo residues 23–33, respectively. Our findings argue that the discrete N-terminal amino acid residues are indispensable for the anterograde and retrograde intracellular movements of PrP^C.

Keywords: Cellular prion protein; Green fluorescent protein; Microtubules; Kinesin family; Dynein

The posttranslational conformational change of the cellular isoform of prion protein (PrP^C) into the scrapie isoform of prion protein (PrP^{Sc}) is the fundamental process underlying the pathogenesis of the prion disease [2,3]. An initial degradation of PrP^C involves cleavage of the NH2-terminal fragment to produce a COOH-terminal 17-kDa polypeptide which was found in a Triton X-100 insoluble fraction [4], of which the cleavage site was mapped at the amino acid residues between the 3F4 (amino acids 108/111 in mouse (Mo) PrP) and the 13A5 (amino acids 138 in Mo PrP) epitopes [4–6]. Several groups reported that NH2-terminal fragment of the PrP functions as a putative targeting element [7,8] and is essential for both transport to the plasma membrane and modulation of endocytosis [9]. GFP-tagged version of PrP^C was found to be properly anchored at the cell surface and its distribution pattern was similar to that of the endogenous PrP^C, with labelling at the plasma membrane and in an intracellular perinuclear compartment [10–14].

We previously demonstrated the microtubule-associated intracellular localization of the NH2-terminal fluorescent PrP^C fragment [1] in Mo neuroblastoma neuro2a (N2a), known to be infectable with PrP^{Sc} [15] and HpL3-4 cells, a hippocampal cell line established from *prnp* gene-ablated mice [16], by utilizing double-labelled PrP^C. At a steady state level, we detected NH_2-terminally fluorescent-tagged PrP^C predominantly in the intracellular compartments, COOH-terminally fluorescent-tagged PrP^C mostly at the cell surface membranes overlapping with lipid rafts, and PrP^C in full length with the merged color in Golgi compartments. The NH_2-terminal PrP^C fragment, which may not reflect the distribution to any single specific organelle, congregated in the cytosol after the treatment with a microtubule

* Corresponding author. Fax: +81-42-346-1748.
E-mail address: kaneko@ncnp.go.jp (K. Kaneko).

0006-291X/$ - see front matter © 2004 Elsevier Inc. All rights reserved.
doi:10.1016/j.bbrc.2004.01.126

depolymerizer (nocodazole). Such microtubule-associated intracellular localization required at least the 1–91 amino acid residues of the NH2-terminal PrP^C fragment.

With this background, we performed a follow-up study of intracellular GFP-PrP^C by a real-time imaging, which demonstrated the anterograde and retrograde intracellular movements of the NH_2-terminal PrP^C fragment in N2a and HpL3-4 cells.

Materials and methods

Construction of GFP-PrP and the deletion mutants. GFP-PrP constructs were made as previously described [1], and the resulted plasmid was designated pSPOX-MHM2PrP::GFP. The series of deletion mutants were amplified by PCR from the pSPOX-MHM2PrP::GFP [1] using 5′-GCA ACC GTT ACC CAC CTC AGG GGG GTA CCC ATA ATC AGT GGA ACA AGC CC-3′ as the forward primer and the following backward primers: 5′-CTG AGG TGG GTA ACG GTT GCC TCC AGG GCT-3′ (for amino acid residues Δ53–91 in Mo PrP), 5′-CTG ATG TCG GCC TCT GCA AAG GTA TGG TGA GC-3′ and 5′-TTT GCA GAG GCC GAC ATC AGT CCA CAT AGT-3′ (Δ23–33), digested with *Bam*HI and *Xho*I, and replaced with the *Bam*HI–*Xho*I fragment of pSPOX-MHM2PrP::GFP [17]. The resulted plasmids were verified by direct DNA sequencing.

Antibodies and drugs. Anti-kinesin and anti-dynein antibodies were purchased from Santa Cruz Biotechnology, and anti-γ-tubulin antibody was purchased from Sigma. Vanadate and AMP-PNP were purchased from CHEMICON and Sigma, respectively. Nocodazole was purchased from Sigma.

Cell cultures, DNA transfection, and drug treatments. Mo neuroblastoma neuro2a (N2a) cells known to be infectable with PrP^{Sc} [15] were obtained from American Tissue Culture Collection. A hippocampal cell line established from *prnp* gene-ablated mice (HpL3-4) was kindly provided by Dr. T. Onodera. Cells were grown and maintained at 37 °C in MEM supplemented with 10% fetal bovine serum. N2a and HpL3-4 cells were transiently transfected with each construct using a DNA transfection kit (Lipofectamin, Gibco-BRL). Western blot analyses were performed as described [17]. Vanadate (10 μM at 30 °C for 30 min) and AMP-PNP (100 μM and 2 mM at 30 °C for 30 min) treatments were performed according to the previous report [18].

Immunofluorescent microscopy. For indirect immunofluorescence analysis, fluorescent PrP^C-transfected N2a cells were rinsed with PBS with Ca^{2+} and Mg^{2+} (PBS(+)) and then fixed with 10% formalin in 70% PBS(+) for 30 min at room temperature. After four washes with PBS(−), the fixed cells were incubated 10% FBS in PBS(−) for 30 min at room temperature. They were then incubated for 1 h at room temperature with antibodies at desired concentrations. After four washes with PBS(−), the cells were incubated with either Alexa488 (green) Fluor-conjugated anti-rabbit IgG (Molecular Probes) or Alexa594 (red) Fluor-conjugated anti-mouse IgG (Molecular Probes), diluted 1:200 in PBS, for 1 h at room temperature. The stained cells were washed four times with PBS(−) and mounted with SLOW FADE (Molecular Probes). Samples were imaged with Delta-Vision microscopy system (Applied Precision), out of focus light of the visualized images was removed by interactive deconvolution.

Real-time imaging. To observe living cells, cells were cultured on glass-bottomed dishes (Matsunami) in culture medium without phenol red at 30 °C. Images of cells were collected with a Delta Vision Microscopy System (Applied Precision) equipped with an Olympus IX70 through a cooled CCD camera (Quantix-LC, Photometrics). Fluorescence signals were visualized using a quad beam splitter (Chroma) and the following excitation and emission filter 525/50 nm (Chroma).

In vitro motility assay. For cytosol preparations, N2a cells were collected from 9 cm × 10 dishes, washed and suspended in four volumes of PBS, homogenized, and ultracentrifuged. After ultracentrifugation at 100,000*g* for 60 min, supernatants were collected and used for these experiments. Alexa 594-labelled tubulin (Molecular Probe) was polymerized in PEM buffer (35 mM Pipes, pH 7.0, 0.5 mM EGTA, and 0.5 mM $MgCl_2$). Polymerized tubulin, recombinant GFP-PrP, and cytosol (1 mg/ml) were mixed and incubated at 30 °C for 5 min in PEM buffer in the presence of 1 mM ATP. After incubation, samples were spread onto glass-bottom dishes and then observed with the Delta Vision Microscopy System (Applied Precision).

Results

The intracellular trafficking of fluorescent PrP^C was investigated through the real-time imaging in living cells

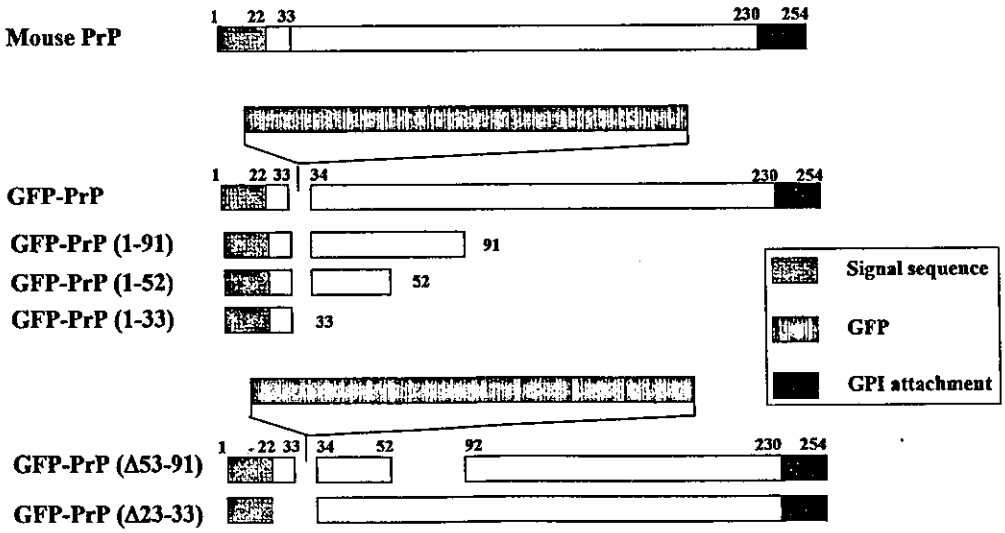

Fig. 1. Immunofluorescent analysis of GFP-PrP^C. The chimeric GFP-PrP constructs including the deletion mutant series used in this study. GFP-PrP (1–91), (1–52), and (1–33) constructs were made as previously described [1]. These recombinant GFP-PrPs were transfected in N2a cells.

by utilizing GFP-PrP constructs (Fig. 1). As results, we revealed that GFP-PrP^C transfected in N2a cells exhibited an anterograde movement towards the direction of plasma membranes at a speed of 140–180 nm/s as well as a retrograde movement inwardly at a speed of 1.0–1.2 μm/s (Fig. 2A). The same results were obtained from other experiments with GFP-PrP^C transfected in HpL3-4 cells (data not shown).

A kinesin family inhibitor of AMP-PNP at a concentration of 100 μM inhibited the anterograde movement of GFP-PrP^C which congregated at an intracellular perinuclear compartment (Fig. 2B), whereas a dynein family inhibitor of vanadate at a concentration of 10 μM inhibited the retrograde movement of GFP-PrP^C which was subsequently detected at the plasma membrane (Fig. 2B) [18]. At a concentration of 2 mM, AMP-PNP inhibited both kinesin and dynein families, and the intracellular motility of GFP-PrP^C was completely blocked (Fig. 2B). The intracellular trafficking of the NH_2-terminal PrP^C fragment was also blocked by the treatment with a microtubule depolymerizer (nocodazole) (data not shown). Furthermore, anti-kinesin antibody (α-kinesin) blocked the anterograde motility of GFP-PrP^C to congregate in an intracellular perinuclear compartment, and anti-dynein antibody (α-dynein) blocked its retrograde motility to reside at a plasma membrane (Fig. 2C).

Next, the deletion mutants (Fig. 1) were used to identify the amino acid residues responsible for the anterograde and retrograde movements of GFP-PrP^C. Truncated constructs with the amino acid residues 1–121, 1–111, and 1–91 in Mo PrP transfected in N2a cells

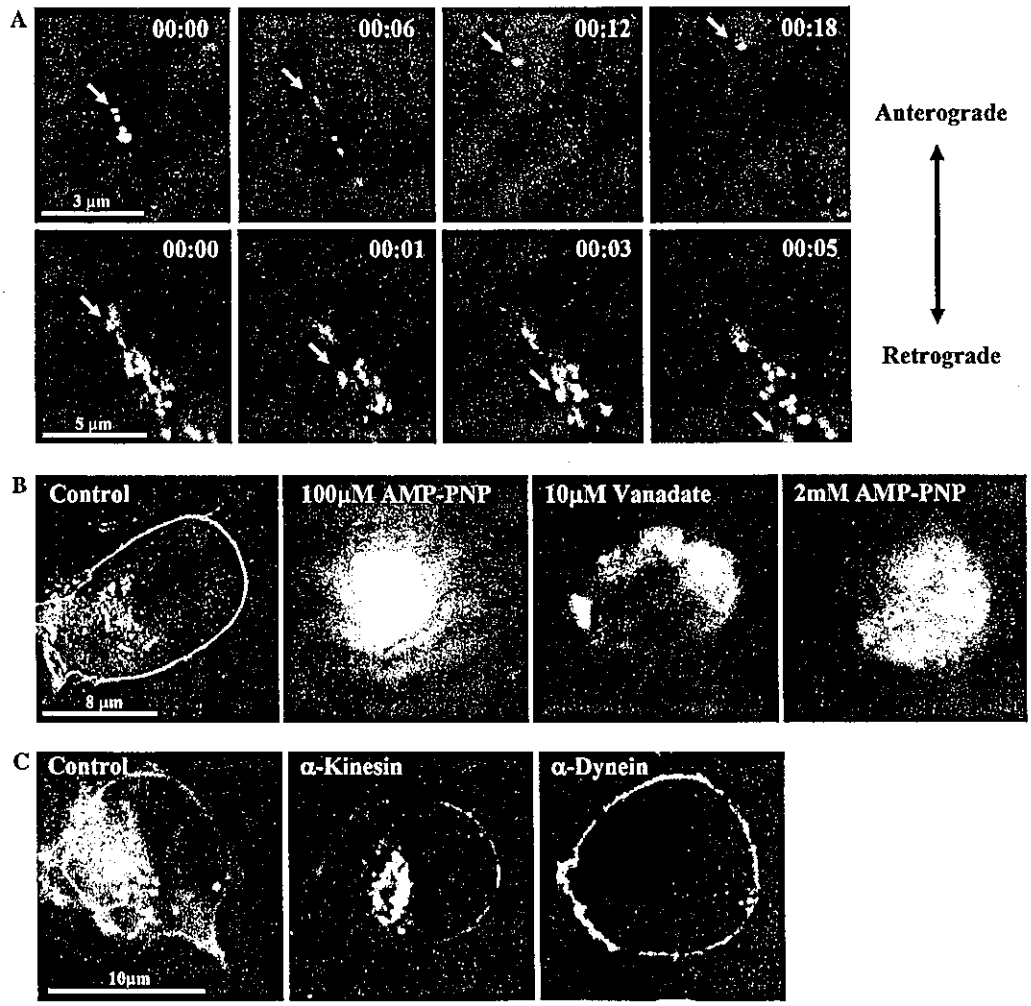

Fig. 2. Intracellular trafficking of GFP-PrP^C by a real-time imaging in living cells, and the drug- or antibody-mediated inhibitions of intracellular movements. (A) Recombinant GFP-PrP^C transfected in N2a cells exhibits an anterograde movement at a speed of 140–180 nm/s (upper panels) and an inward retrograde movement at a speed of 1.0–1.2 μm/s (lower panels). Scale bar (upper panel) = 3 μm and scale bar (lower panel) = 5 μm. (B) A kinesin family inhibitor of AMP-PNP at a concentration of 100 μM inhibited the anterograde movement of GFP-PrP^C which congregates in an intracellular perinuclear compartment. A dynein family inhibitor of vanadate at a concentration of 10 μM inhibits the retrograde movement of GFP-PrP^C which congregates at a plasma membrane. At a concentration of 2 mM, AMP-PNP inhibits both kinesin and dynein families, and the intracellular motility of GFP-PrP^C is completely blocked. Scale bar = 8 μm. (C) Anti-kinesin antibody (α-kinesin) blocks the anterograde motility of GFP-PrP^C and anti-dynein antibody (α-dynein) blocks its retrograde motility.

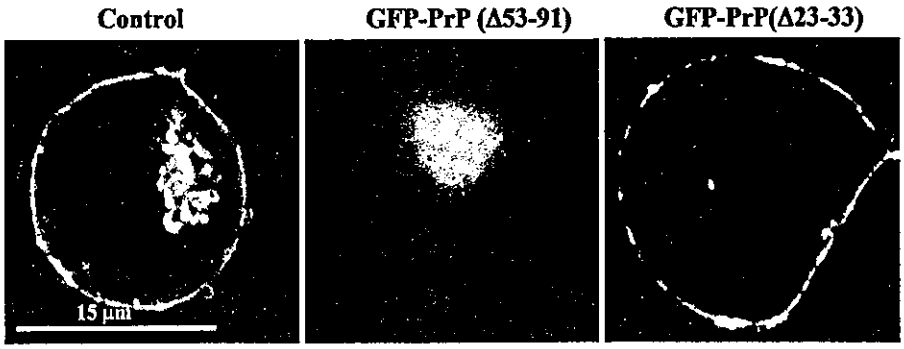

Fig. 3. The amino acid residues responsible for the anterograde and retrograde movements of GFP-PrP^C. The truncated construct of GFP-PrP lacking the amino acid residues 53–91 in Mo PrP loses its anterograde motility and congregates in the intracellular perinuclear compartment. The GFP-PrP construct lacking the amino acid residues 23–33 in Mo PrP loses its retrograde motility and resides at the plasma membrane. Scale bar = 15 μm.

exhibited its proper anterograde and retrograde motilities (data not shown), whereas those with amino acid residues 1–52 and 1–33 in Mo PrP did not [1]. These truncated GFP-PrP^C (1–33 and 1–52) surrounded the γ-tubulin-positive centrosome (microtubule organizing center) (data not shown), suggesting that the truncated GFP-PrP^C with at most 1–52 lost its anterograde movement but those with at least 1–33 still exhibited the dynein-driven retrograde movement. Thus, discrete amino acid residues 53–91 and 23–33 (the first NH2-terminal 1–22 amino acid residues act as a signal sequence) seem to be indispensable for the anterograde and retrograde movements, respectively. In accordance with these observations, the deletion constructs lacking the amino acid residues 53–91 in Mo PrP (GFP-PrP^C (Δ53–91)) lost its anterograde motility and congregated in an intracellular perinuclear compartment, whereas those lacking the amino acid residues 23–33 (GFP-PrP^C (Δ23–33)) lost its retrograde motility and resided at a plasma membrane (Fig. 3).

Finally, an in vitro motility assay [19] was further performed to obtain direct evidence on the interaction at the cytosolic interface between recombinant GFP-PrP and Alexa 594-labelled microtubules with or without cytosolic fractions including kinesin family and dynein motor proteins. However, no movement of GFP-PrP along Alexa 594-labelled microtubules was observed even after the addition of cytosolic fractions (Fig. 4).

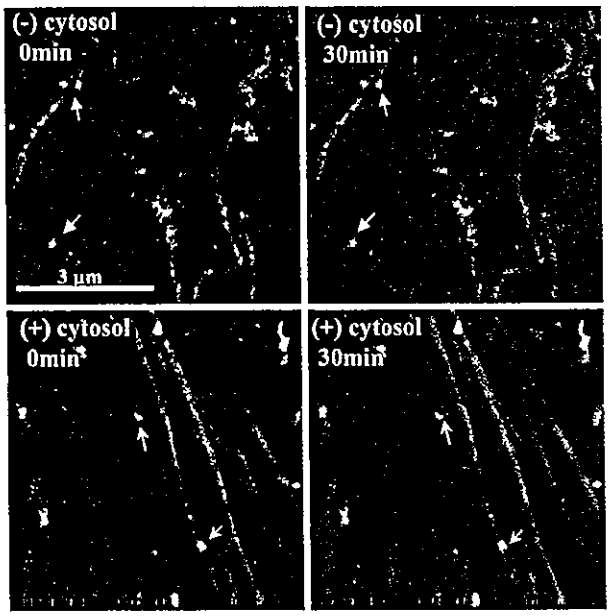

Fig. 4. In vitro motility assay of recombinant GFP-PrP. Polymerized Alexa 594-labelled tubulin, recombinant GFP-PrP, and cytosol (1 mg/ml) were incubated at 30 °C for 5 min in the presence of 1 mM ATP. No movement of recombinant GFP-PrP (arrow heads) along Alexa 594-labelled microtubules was observed for 0–30 min even after the addition of cytosolic fractions (cytosol). Scale bar = 3 μm.

Discussion

We previously reported the microtubule-associated intracellular localization of NH2-terminal PrP^C fragment at a steady state level [1]. A real-time imaging of GFP-PrP^C in living cells, however, has been awaited for further understanding its dynamics along the microtubular network.

Microtubules are essential and ubiquitous cytoskeletal elements composed of heterodimers of α- and β-tubulin, and serve many vital roles, participating in organization of the cytoplasm, in cell motility, and in mitosis [20,21]. In addition to tubulin itself, several microtubule-associated proteins (MAPs) comprise cellular microtubules. The molecular motors that move along microtubules have two origins. The kinesin and myosin families of ATPase motors share a common core structure and may have the same common ancestor as the GTPases involved in signalling and protein synthesis [20,22]. Dynein is part of the family of AAA ATPases [23] that also contribute to protein folding (Hsp100 chaperones), membrane traffic (*N*-ethylmaleimide-sensitive factor or NSF), and DNA synthesis (clamp loader proteins).

Here we showed the anterograde transport of GFP-PrP^C at a speed of 140–180 nm/s and the retrograde transport at a speed of 1.0–1.2 μm/s. These anterograde and retrograde transports of GFP-PrP^C were completely inhibited by AMP-PNP/vanadate which stop the kinesin family/dynein family-driven movements, respectively. Furthermore, anti-kinesin antibody (α-kinesin) blocked the anterograde motility of GFP-PrP^C, and anti-dynein antibody (α-dynein) blocked its retrograde motility. Among the kinesin superfamily, KIF4 moves latex beads from the minus to the plus ends of microtubules, a direction that corresponds to anterograde transport in the axon at a speed of <200 nm/s [24], and dynein is the force-generating protein that produces force in the direction corresponding to retrograde organelle transport at a speed of about 1.4 μm/s in the cell [25–28]. Thus, the anterograde transport of intracellular GFP-PrP^C might be compatible with the speed of the KIF4-driven movement, while the retrograde movement is compatible with that of the dynein-driven movement.

Mapping of the distinct kinesin family-interacting domain and the dynein-interacting domain identified the minimum required amino acid residues in the NH2-terminal PrP^C fragment. The kinesin family-interacting domain (Mo 53–91) is overlapped with an octapeptide repeat region, which is related to the copper metabolism [29–33]. In terms of the PrP^{Sc} formation, the C-terminal domain of PrP^C is known to be insufficient to impede the conversion of the full-length PrP^C molecule to PrP^{Sc} and N-terminally truncated molecules (with residues 23–88 and 23–120 deleted) have reduced dominant-negative activity, and the extreme N-terminal sequence (23KKRPKP29) enhances the dominant-negative phenotype on the formation of PrP^{Sc} [34,35]. This basic sequence is highly conserved in all species studied to date [36]. On the other hand, deletion of the octarepeat sequences (residues 52–91) did not alter PrP^{Sc} formation and dominant-negative inhibition on the formation of PrP^{Sc} [35]. The relevance of these observations to the intracellular trafficking of PrP^C needs to be further investigated.

After internalized, the NH2-terminal PrP^C fragment seems to reside inside vesicles where integral membrane proteins and linker proteins in some cases would be required for the interaction with microtubules to bridge the luminal and cytoplasmic phases across the membranes [1]. Thus, it seems less likely that PrP^C is engaged in the direct interaction with the motor molecules, which is compatible with the fact that the in vitro motility assay failed to show that recombinant GFP-PrP directly moved along Alexa 594-labelled microtubules.

It is also important to identify how many NH2-terminal PrP^C fragments reside in each PrP^C-positive vesicle. In order to answer this question, a single fluorescent molecule is a good potential source because it can emit only one photon at a time. Otherwise it is indispensable to utilize a technique which allows us to know how many photons emit from each PrP^C molecule. Unfortunately, we are currently unable to utilize these techniques. Nonetheless, our results shed a new right on the mechanisms underlying the intracellular trafficking of PrP^C.

Acknowledgments

We greatly thank T. Onodera for providing us the HpL3-4 cell line, E. Nannri, K. Ishibashi, C. Ota, and Y. Yamaura for technical assistance. This work was supported by grants from the Core Research for Evolutional Science and Technology (CREST) of Japan Science and Technology Corporation, Health and Labour Sciences Research Grants, Research on Advanced Medical Technology, nano-001, and the Ministry of Health, Labor and Welfare of Japan.

References

[1] N. Hachiya, K. Watanabe, Y. Sakasegawa, K. Kaneko, Microtubules-associated intracellular localization of the NH2-terminal cellular prion protein fragment, Biochem. Biophys. Res. Commun. 313 (2004) 818–823.
[2] S.B. Prusiner, D.C. Bolton, D.F. Groth, K.A. Bowman, S.P. Cochran, M.P. McKinley, Further purification and characterization of scrapie prions, Biochemistry 21 (1982) 6942–6950.
[3] S.B. Prusiner, P. Peters, K. Kaneko, A. Taraboulos, V. Lingappa, F.E. Cohen, S.J. DeArmond, Cell Biology of Prions, Cold Spring Harbor, New York, 1999.
[4] A. Taraboulos, M. Scott, A. Semenov, D. Avrahami, L. Laszlo, S.B. Prusiner, Cholesterol depletion and modification of COOH-terminal targeting sequence of the prion protein inhibit formation of the scrapie isoform, J. Cell Biol. 129 (1995) 121–132.
[5] M. Rogers, D. Serban, T. Gyuris, M. Scott, T. Torchia, S.B. Prusiner, Epitope mapping of the Syrian hamster prion protein utilizing chimeric and mutant genes in a vaccinia virus expression system, J. Immunol. 147 (1991) 3568–3574.
[6] K.-M. Pan, N. Stahl, S.B. Prusiner, Purification and properties of the cellular prion protein from Syrian hamster brain, Protein Sci. 1 (1992) 1343–1352.
[7] S.-L. Shyng, J.E. Heuser, D.A. Harris, A glycolipid-anchored prion protein is endocytosed via clathrin-coated pits, J. Cell Biol. 125 (1994) 1239–1250.
[8] S.-L. Shyng, K.L. Moulder, A. Lesko, D.A. Harris, The N-terminal domain of a glycolipid-anchored prion protein is essential for its endocytosis via clathrin-coated pits, J. Biol. Chem. 270 (1995) 14793–14800.
[9] M. Nunziante, S. Gilch, H.M. Schatzl, Essential role of the prion protein N terminus in subcellular trafficking and half-life of cellular prion protein, J. Biol. Chem. 278 (2003) 3726–3734.
[10] K.S. Lee, A.C. Magalhaes, S.M. Zanata, R.R. Brentani, V.R. Martins, M.A. Prado, Internalization of mammalian fluorescent cellular prion protein and N-terminal deletion mutants in living cells, J. Neurochem. 79 (2001) 79–87.
[11] A.C. Magalhaes, J.A. Silva, K.S. Lee, V.R. Martins, V.F. Prado, S.S.G. Ferguson, M.V. Gomez, R.R. Brentani, M.A.M. Prado, Endocytic intermediates involved with the intracellular trafficking of a fluorescent cellular prion protein, J. Biol. Chem. 277 (2002) 33311–33318.
[12] A. Negro, C. Ballarin, A. Bertoli, M.L. Massimino, M.C. Sorgato, The metabolism and imaging in live cells of the bovine prion

protein in its native form or carrying single amino acid substitutions, Mol. Cell. Neurosci. 17 (2001) 521–538.
[13] H. Lorenz, O. Windl, H.A. Kretzschmar, Cellular phenotyping of secretory and nuclear prion proteins associated with inherited prion diseases, J. Biol. Chem. 277 (2002) 8508–8516.
[14] L. Ivanova, S. Barmada, T. Kummer, D.A. Harris, Mutant prion proteins are partially retained in the endoplasmic reticulum, J. Biol. Chem. 276 (2001) 42409–42421.
[15] D.A. Butler, M.A. Scott, J.M. Bockman, D.R. Borchelt, A. Taraboulos, K.K. Hsiao, D.T. Kingsbury, S.B. Prusiner, Scrapie-infected murine neuroblastoma cells produce protease-resistant prion proteins, J. Virol. 62 (1988) 1558–1564.
[16] C. Kuwahara, A.M. Takeuchi, T. Nishimura, K. Haraguchi, A. Kubosaki, Y. Matsumoto, K. Saeki, T. Yokoyama, S. Itohara, T. Onodera, Prions prevent neuronal cell-line death, Nature 400 (1999) 225–226.
[17] M.R. Scott, R. Kohler, D. Foster, S.B. Prusiner, Chimeric prion protein expression in cultured cells and transgenic mice, Protein Sci. 1 (1992) 986–997.
[18] T.A. Schroer, M.P. Sheetz, Role of kinesin and kinesin-associated proteins in organelle transport, in: F.D. Warner, J.R. McIntosh (Eds.), Cell Movement, Alan R. Liss, New York, 1989, pp. 295–306.
[19] A. Kubo, H. Sasaki, A. Yuba-Kubo, S. Tsukita, N. Shiina, Centriolar satellites: molecular characterization, ATP-dependent movement toward centrioles and possible involvement in ciliogenesis, J. Cell Biol. 147 (1999) 969–980.
[20] T.D. Pollard, The cytoskeleton, cellular motility and the reductionist agenda, Nature 422 (2003) 741–745.
[21] J. Howard, A.A. Hyman, Dynamics and mechanics of the microtubule plus end, Nature 422 (2003) 753–758.
[22] R.D. Vale, R.A. Milligan, The way things move: looking under the hood of molecular motor proteins, Science 288 (2000) 88–95.
[23] G. Mocz, I.R. Gibbons, Model for the motor component of dynein heavy chain based on homology to the AAA family of oligomeric ATPases, Structure (Camb) 9 (2001) 93–103.
[24] N. Hirokawa, Kinesin and dynein superfamily proteins and the mechanism of organelle transport, Science 279 (1998) 519–526.
[25] R.D. Vale, B.J. Schnapp, T. Mitchison, E. Steuer, T.S. Reese, M.P. Sheetz, Different axoplasmic proteins generate movement in opposite directions along microtubules in vitro, Cell 43 (1985) 623–632.
[26] R.D. Vale, T.S. Reese, M.P. Sheetz, Identification of a novel force-generating protein, kinesin, involved in microtubule-based motility, Cell 42 (1985) 39–50.
[27] B.M. Paschal, R.B. Vallee, Retrograde transport by the microtubule-associated protein MAP 1C, Nature 330 (1987) 181–183.
[28] R.B. Vallee, J.S. Wall, B.M. Paschal, H.S. Shpetner, Microtubule-associated protein 1C from brain is a two-headed cytosolic dynein, Nature 332 (1988) 561–563.
[29] D.R. Brown, K. Qin, J.W. Herms, A. Madlung, J. Manson, R. Strome, P.E. Fraser, T. Kruck, A. von Bohlen, W. Schulz-Schaeffer, A. Giese, D. Westaway, H. Kretzschmar, The cellular prion protein binds copper in vivo, Nature 390 (1997) 684–687.
[30] P.C. Pauly, D.A. Harris, Copper stimulates endocytosis of the prion protein, J. Biol. Chem. 273 (1998) 33107–33110.
[31] M.L. Kramer, H.D. Kratzin, B. Schmidt, A. Romer, O. Windl, S. Liemann, S. Hornemann, H. Kretzschmar, Prion protein binds copper within the physiological concentration range, J. Biol. Chem. 276 (2001) 16711–16719.
[32] W.S. Perera, N.M. Hooper, Ablation of the metal ion-induced endocytosis of the prion protein by disease-associated mutation of the octarepeat region, Curr. Biol. 11 (2001) 519–523.
[33] A.P. Garnett, J.H. Viles, Copper binding to the octarepeats of the prion protein. Affinity, specificity, folding, and cooperativity: insights from circular dichroism, J. Biol. Chem. 278 (2003) 6795–6802.
[34] K. Kaneko, L. Zulianello, M. Scott, C.M. Cooper, A.C. Wallace, T.L. James, F.E. Cohen, S.B. Prusiner, Evidence for protein X binding to a discontinuous epitope on the cellular prion protein during scrapie prion propagation, Proc. Natl. Acad. Sci. USA 94 (1997) 10069–10074.
[35] L. Zulianello, K. Kaneko, M. Scott, S. Erpel, D. Han, F.E. Cohen, S.B. Prusiner, Dominant-negative inhibition of prion formation diminished by deletion mutagenesis of the prion protein [In Process Citation], J. Virol. 74 (2000) 4351–4360.
[36] P. Bamborough, H. Wille, G.C. Telling, F. Yehiely, S.B. Prusiner, F.E. Cohen, Prion protein structure and scrapie replication: theoretical, spectroscopic, and genetic investigations, Cold Spring Harb. Symp. Quant. Biol. 61 (1996) 495–509.

Non-glycosylphosphatidylinositol (GPI)-anchored recombinant prion protein with dominant-negative mutation inhibits PrP^{Sc} replication *in vitro*

Hitaru Kishida[1,2], Yuji Sakasegawa[1,3], Kota Watanabe[1,3], Yoshio Yamakawa[4], Masahiro Nishijima[4], Yoshiyuki Kuroiwa[2], Naomi S. Hachiya[1,3] and Kiyotoshi Kaneko[1,3]

1. Department of Cortical Function Disorders, National Institute of Neuroscience, National Center of Neurology and Psychiatry, Kodaira, Tokyo, Japan
2. Department of Neurology, Yokohama City University, Yokohama, Japan
3. Core Research for Evolutional Science and Technology (CREST), Japan Science and Technology Corporation, Kawagoe, Saitama, Japan
4. Department of Biochemistry and Cell Biology, National Institute of Infectious Diseases, Tokyo, Japan

Key Words: recombinant prion protein (rPrP), dominant negatives, Q218K, quinacrine, glycosylphosphatidylinositol (GPI)-anchor, lipid rafts, Creutzfeldt-Jakob disease (CJD)

Abbreviations: PrP = prion protein, GPI = glycosylphosphatidylinositol, CJD = Creutzfeldt-Jakob disease, rPrP = recombinant prion protein, EC_{50} = 50% effective concentration, EC_{99} = 99% effective concentration, PrP^{C} = host-encoded cellular prion protein, PrP^{Sc} = abnormal protease-resistant pathogenic prion protein, TSE = transmissible spongiform encephalopathy, BSE = bovine spongiform encephalopathy, IPTG = Isopropyl-β-D-thiogalactopyranoside, β-ME = β-mercaptoethanol, PMSF = Phenylmethylsulfonyl fluoride, PBS = phosphate buffer saline, PK = proteinase K, WST-8 = 2- (2-methoxy-4-nitrophenyl)- 3- (4-nitrophenyl)- 5- (2,4-disulfophenyl)- 2H- tetrazolium, monosodium salt, SPR = surface plasmon resonance, PIPLC = phosphatidyl-inositol specific phospholipase C

Abstract

Dominant-negative mouse prion protein (PrP) with a lysine mutation at codon 218 (Q218K) is known to inhibit prion replication. In order to gain further mechanistic insight into such dominant negative inhibition, non-glycosylphosphatidylinositol (GPI)-anchored recombinant PrP with Q218K (rPrP-Q218K) was investigated. When applied into scrapie-infected mouse neuroblastoma (ScN2a) cells, rPrP-Q218K but not wild-type rPrP (rPrP-WT) exclusively inhibited abnormal protease-resistant pathogenic isoform (PrP^{Sc}) replication without reducing the viability of the cells. It was even more efficient than quinacrine, which has already been prescribed for sporadic Creutzfeldt-Jakob disease (CJD) patients; 50% effective concentration (EC_{50}) = 0.20 μM, 99% effective concentration (EC_{99}) = 0.86 μM vs. EC_{50} = 0.45 μM, EC_{99} = 1.5 μM. Besides, no apparent cell damage was observed at the concentration of up to 4.3 μM (100 μg/ml). In combination treatment with 0.43 μM (10 μg/ml) of rPrP-Q218K, EC_{99} of quinacrine was decreased from 1.5 μM to 0.5 μM, and the cell viability was recovered from 50% to over 90% as inversely proportional to the concentration of quinacrine. Such combination could alleviate the side effects of quinacrine by reducing its effective concentration without changing or even acceleration the inhibition efficacy. Since homogeneous, high-quality rPrPs could be easily prepared from Escherichia coli in large quantities, rPrP-Q218K is a good candidate for a prion replication antagonist.

Correspondence: Dr. Kiyotoshi Kaneko, MD, Department of Cortical Function Disorders, National Institute of Neuroscience, National Center of Neurology and Psychiatry, 4-1-1 Ogawahigashi Kodaira, Tokyo 187-8502, Japan
Tel: 81-42-346-1718 Fax: 81-42-346-1748 E-mail: kaneko@ncnp.go.jp

Submitted: July 14, 2003 Revision Accepted: October 22, 2003

DOI: 10.1080/13506120410001689634

Introduction

Human prion disease or transmissible spongiform encephalopathy (TSE), such as sporadic Creutzfeldt-Jakob disease (CJD) and variant CJD transmitted from bovine spongiform encephalopathy (BSE) constitutes a group of invariably fatal neurodegenerative disorders[1,2]. Prion protein (PrP) consists of two isoforms, one is a host-encoded cellular isoform (PrP^{C}) and the other is an abnormal protease-resistant pathogenic isoform (PrP^{Sc}). The latter is a causative agent of prion disease. PrP^{Sc} stimulates the conversion of PrP^{C} into nascent PrP^{Sc}, and the accumulation of PrP^{Sc} leads to the central nervous system (CNS) dysfunction and neuronal degeneration[3].

A human polymorphic lysine variant at codon 219 (E219K) in the Japanese population, known to render humans resistant to sporadic CJD[4,5], acts as a dominant negative in scrapie-infected mouse neuroblastoma (ScN2a) culture cells after gene transfection[6,7] and transgenic mice expressing lysine at codon 218 in mouse PrP (mouse Q218K, which corresponds to human E219K)[8]. Of note, such a genetic population with E219K and the transgenic mice with Q218K complete their life span with no apparent phenotypic abnormality[5,8].

We now demonstrate that administration of non-glycosylphosphatidylinositol (GPI)-anchored recombinant PrP (rPrP) with Q218K mutation (rPrP-Q218K) but not wild-type rPrP (rPrP-WT) exclusively inhibited the PrP^{Sc} formation in ScN2a cells, even more efficiently than quinacrine, which has already been prescribed for CJD patients, and no apparent cell damage was observed up to 5-fold higher concentrations of a 99% effective concentration (EC_{99}). When combined, rPrP-Q218K efficiently reduced the effective dosage of quinacrine, and thus rendered ScN2a culture cells more viable. Such a combination could alleviate the side effects of quinacrine by reducing its effective concentration without changing or even accelerating the inhibition efficacy. Since homogeneous, high-quality rPrP could be easily prepared from *Escherichia coli* in large quantities, rPrP-Q218K might be a good candidate as a prion replication antagonist.

Materials and methods

Expression plasmid construction

The gene, mouse (Mo) PrP(23-230), coding for residues 23-230 of mouse PrP was PCR-amplified from mouse brain cDNA using the oligonucleotide primers (5′-GGAATTCACCATGAAAAAGCGGCCAAAGCCTGGAGGG-3′ and 5′-CCGCTCGAGTCAGGATCTTCTCCCGTCGTAATAGGC-3′) and cloned via *EcoRI* and *XhoI* sites into the plasmid pBluescript II SK(+) (Stratagene, La Jolla, CA). The genes for 3F4-tagged MoPrP (MHM2PrP) were also cloned using PCR amplification from pSPOX-MHM2PrP[9,10] as above. The Q218K mutation was generated by PCR-directed mutagenesis using primers (5′-ATGTGCGTCACCCAGTACAAAAAGGAGTCC-3′ and 5′-ATAGGCCTGGGACTCCTTTTTGTACTGGGT-3′). The DNA fragments were cloned into a modified pET-11a (Invitrogen, Carlsbad, CA), pEY2, of which *EcoRI* and *XhoI* sites were introduced as multicloning sites, via *EcoRI* and *XhoI* sites.

Purification of recombinant prion proteins (rPrPs)

The rPrPs were expressed as inclusion bodies in the *E. coli* BL21(DE3) (Stratagene) in the presence of 0.1 mM Isopropyl-β-D-thiogalactopyranoside (IPTG). The inclusion bodies were collected from sonicated lysates by centrifugation at 27,000 × g for 10 min, washed three times in Buffer A (2 M urea, 50 mM Tris-HCl, pH 7.5, 150 mM NaCl, 2 mM β-mercaptoethanol (β-ME), 0.5 mM Phenylmethylsulfonyl fluoride (PMSF)), and solubilized in Buffer B (8 M urea, 25 mM Tris-HCl, pH 7.5, 2 mM β-ME, 0.5 mM PMSF). After centrifugation (200,000 × g, 30 min), the supernatant was applied to a CM-Sepharose column (Amersham Bioscience, Piscataway, NJ), washed with Buffer B containing 100 mM NaCl and eluted with Buffer B containing 150 mM NaCl. The eluate containing rPrP was applied to an Ni-NTA agarose column (Qiagen, Valencia, CA), washed with Buffer B containing 5 mM imidazole and eluted with Buffer B containing 200 mM imidazole. The eluate was diluted 10-fold 1 M arginine-HCl, pH 8.0, 1 mM reduced glutathione, 0.8 mM oxidized glutathione and incubated at 4°C overnight. After incubation at 37°C for 10 min, the refolded recombinant proteins were concentrated and buffer-changed into phosphate buffer saline (PBS) by Ultrafree-15 10K NMWL (Millipore, Billerica, MA). Concentrations of rPrP were calculated by the absorbance at 280 nm with specific absorbance unit ($A_{280nm,\ 1mg/ml,\ 1cm}$) of 2.70.

Inhibition assay of PrP^{Sc} accumulation in ScN2a cells

ScN2a cells were grown and maintained as described[11]. Twenty-four hours after splitting, cells were incubated in a fresh medium containing the appropriate concentration of rPrP and/or quinacrine (Sigma, St. Louis, MO) or the same volume of PBS as a negative control and incubated for 3 days. Quinacrine was dissolved in PBS. Cell lysis and proteinase K (PK) digestion were performed as described[12]. PK-insoluble pellets and PK-undigested samples were subjected to 12% SDS-PAGE and Western blotting using standard procedure. Anti-PrP